SOLUBLE ALKYL SUBSTITUTED POLY(3,4PROPYLENEDIOXYSELENOPHNE)S: A NOVEL PLATFORM FOR OPTOELECTRONIC MATERIALS

A THESIS SUBMITTED TO
THE GRADUATE SCHOOL OF NATURAL AND APPLIED SCIENCES
OF
MIDDLE EAST TECHNICAL UNIVERSITY

BY

SAMED ATAK

IN PARTIAL FULFILLMENT OF THE REQUIREMENTS
FOR
THE DEGREE OF MASTER OF SCIENCE
IN
POLYMER SCIENCE AND TECHNOLOGY

MARCH 2011

Approval of the thesis:

SOLUBLE ALKYL SUBSTITUTED POLY(3,4PROPYLENEDIOXYSELENOPHNE)S: A NOVEL PLATFORM FOR OPTOELECTRONIC MATERIALS

submitted by **SAMED ATAK** in partial fulfillment of the requirements for the degree of **Master of Science in Polymer Science and Technology Department, Middle East Technical University** by,

Prof. Dr. Canan Özgen
Dean, Graduate School of **Natural and Applied Sciences** _____

Prof. Dr. Necati Özkan
Head of Department, **Polymer Science and Technology** _____

Prof. Dr. Ahmet M. Önal
Supervisor, **Polymer Science and Tech. Dept., METU** _____

Assoc. Prof. Dr. Atilla Cihaner
Co-Supervisor, **Chemical Engineering and Applied Chemistry Dept., ATILIM UNIVERSITY** _____

Examining Committee Members:

Prof. Dr. Zuhal Küçükyavuz _____
Polymer Science and Technology Dept., METU

Prof. Dr. Ahmet Muhtar Önal _____
Polymer Science and Technology Dept., METU

Prof. Dr. Teoman Tinçer _____
Polymer Science and Technology Dept., METU

Assoc. Prof. Dr. Atilla Cihaner _____
Chemical Engineering and
Applied Chemistry Dept., ATILIM UNIVERSITY

Assist. Prof. Dr. Ali Çirpan _____
Polymer Science and Technology Dept., METU

Date: March 18, 2011

I hereby declare that all information in this document has been obtained and presented in accordance with academic rules and ethical conduct. I also declare that, as required by these rules and conduct, I have fully cited and referenced all materials and results that are not original to this work.

Name, Last name: Samed, Atak

Signature:

ABSTRACT

SOLUBLE ALKYL SUBSTITUTED
POLY(3,4PROPYLENEDIOXYSELENOPHNE)S:
A NOVEL PLATFORM FOR OPTOELECTRONIC MATERIALS

Atak, Samed

M.Sc., Department of Polymer Science and Technology

Supervisor: Prof. Dr. Ahmet M. Önal

Co-Supervisor: Assoc. Prof. Dr. Atilla Cihaner

March 2011, 76 pages

In this study, optical and electrochemical properties of regioregular and soluble alkyl substituted propylenedioxyselenophene based electrochromic polymers, namely poly(3,3-dibutyl-3,4-dihydro-2H-selenopheno[3,4-b][1,4]dioxephine) (PProDOS-C_4), poly(3,3-dihexyl-3,4-dihydro-2H-selenopheno[3,4-b][1,4]dioxephine) (PProDOS-C_6), and poly(3,3-didecyl-3,4-dihydro-2H-selenopheno[3,4-b][1,4]dioxephine) (PProDOS-C_{10}), which were synthesized via electrochemical polymerization, were investigated. It is noted that these unique polymers have low band gaps (1.54 – 1.64 eV) and they are exceptionally stable under ambient atmospheric conditions. For example, polymer films retained 84-96 % of their electroactivity after five thousands cycles. The percent transmittance of PProDOS-C_n (n= 4, 6, 10) films found to be between 55-59 %. Furthermore, these novel soluble PProDOS-C_n polymers showed electrochromic behavior: a color change form pure blue (L = 57.31, a = -13.18, b = - 42.68) to highly transparent state (L = 91.74, a = 2.52, b = -1.30) state in a low switching time (1.0 s) during oxidation with high coloration efficiencies (328 – 864 cm^2/C) when compared to their close analogues.

Keywords: Conjugated polymers, Polyselenophenes and its derivatives, propylenedioxyselenophenes, ProDOS.

ÖZ

ÇÖZÜNÜR ALKİL SÜBSTİTÜELİ
POLİ(3,4-PROPİLENDİOKSİSELENOFENLER) :
OPTOELEKTRONİK MALZEMELER İÇİN YENİ BİR PLATFORM

Atak, Samed
Y. Lisans, Polimer Bilimi ve Teknolojisi Bölümü
Tez Yöneticisi: Prof. Dr. Ahmet M. Önal
Ortak Tez Yöneticisi: Doç. Dr. Atilla Cihaner

Mart 2011, 76 sayfa

Bu çalışmada, elektokimyasal polimerizasyonla sentezlenen düzenli ve çözünür alkil sübstitüeli propilendioksiselenofen temelli polimerlerin, poli(3,3-dibütil-3,4-dihidro-2H-selenofen[3,4-b][1,4]dioksefin) (PProDOS-C_4), poli(3,3-dihekzil-3,4-dihidro-2H-selenofen[3,4-b][1,4]dioksefin) (PProDOS-C_6), ve poli(3,3-didesil-3,4-dihidro-2H-selenofen[3,4-b][1,4]dioksefin) (PProDOS-C_{10}), optik ve elektrokimyasal özellikleri incelenmiştir. Elde edilen polimerlerin düşük bant aralığına sahip oldukları (1.54-1.64 eV) ve atmosferik koşullarda kararlı oldukları bulunmuştur. Örneğin, polimer filmlerin 5000 döngüden sonra bile % 84-96 arası elektro-etkinliklerini koruduğu gözlenmiştir. PProDOS-C_n (n = 4, 6, 10) polimer filmlerin yüzde geçirgenlikleri %55-59 arası olarak bulunmuştur. Bu yeni çözünebilir polimer filmerin yükseltgenme sırasında mavi renkten (L = 57.31, a = -13.18, b = -42.68) oldukça geçirgen (renksiz) hale (L = 91.74, a = 2.52, b = -1.30) dönüşen elektrokromik özellik gösterdiği ve bu dönüşümü kısa bir anahtarlanma süresinde (1.0 s) yüksek renk etkinliği (328-864 cm^2/C) ile gerçekleştirmektedir.

Anahtar Sözcükler: Konjüge Polimerler, Poliselenofenler ve Türevleri, Propilendioksiselenofenler, ProDOS.

To My Family …

ACKNOWLEDGEMENTS

I would like to express my deepest gratitude to my supervisor Prof. Dr. Ahmet M. ÖNAL and my co-supervisor Dr. Atilla CİHANER starting from the first day, they responded me very politely and always encouraged me with their positive attitude. I sincerely appreciate the time and efforts they have taken to train me and improve my thesis.

I am grateful to Merve İçli ÖZKUT for supporting and criticizing to help doing my best in almost every stage of this work.

I am also thankful to my laboratory friends from 'Prof. Dr. Ahmet M. Önal Research Group' and Buket ÇARBAŞ for their patience and politeness during my study.

I sincerely acknowledge my friends; Fırat HACIOĞLU, Koray CENGİZ, Can NEBİGİL, Merve BEKARLAR, Melek SERMİN, Can SEÇKİN, Tufan ŞAHİN, Emre ERCİYES, Sinan ÇANKAYA and Esin İBİBİKCAN with whom I had spent most of time after working hours when preparing my thesis.

Grateful thanks go to Gizem ELİUZ for her moral support. Without her encouragement and love I could not have finished my M.Sc. program.

I would like to extend my gratitude to my family for their endless love and support in every step of my life. I could not achieve any of these without their support and belief in me.

Finally, I want to thank the Scientific and Technical Research Council of Turkey (TUBITAK-110T564), European Cooperation in Science and Technology (COST-108T959), METU-Chemistry Department, Atılım University (ATÜ-BAP-1011-01) and The Turkish Academy of Sciences (TÜBA) for their financial supports.

TABLE OF CONTENTS

LIST OF FIGURES

FIGURES

LIST OF TABLES

TABLES

LIST OF ABBREVIATIONS

ACN	Acetonitrile
CB	Conduction Band
CP	Conjugated Polymer
CE	Coloration Efficiency
CV	Cyclic Voltammetry
DAD	Donor Acceptor Donor
DCM	Dichloromethane
FTIR	Fourier Transform Infrared Spectroscopy
HOMO	Highest Occupied Molecular Orbital
ITO	Indium-tin oxide
LUMO	Lowest Unoccupied Molecular Orbital
NMR	Nuclear Magnetic Resonance
PEDOS	Poly(3,4-ethylenedioxyselenophene)
PEDOT	Poly(3,4-ethylenedioxythiophene)
ProDOS	Propylenedioxyselenophene
Pt	Platinum
PSe	Polyselenophene
PTh	Polythiophene
RE	Reference Electrode
rt	Room Temperature
SPEL	Spectroelectrochemical
TBAH	Tetrabuthylammoniumhexaflourophosphate
THF	Tetrahyrofuran
VB	Valence Band
UV-VIS	Ultraviolet Visible
WE	Working Electrode
Δ%T	Percent Trasnmittance Changes
Δ%Y	Relative Luminance

CHAPTER 1

INTRODUCTION

1.1. Electrochromism

Electrochromism is basically defined as the reversible color change during the oxidation or reduction by an external potential. The thermochromism (change in color generated by heat) and photochromism (change in color generated by light) are the close term of electrochromism [1]. In general, the color change is observed between transmissive (doped) and colored states (undoped), however, some materials can be switched between multiple colors, called multielectrochromic materials. Inorganic compounds (e.g., tungsten oxide, WO_3, Prussian blue) and conjugated polymers (CPs) are mostly used as electrochromic materials [2-5]. WO_3 was the first well-considered material in the field of electrochromism in 1969 [6]. In fact nowadays, most of the studies about electrochromism have been focused on CPs because they offer better electrochromic properties (low switching time, high contrast ratio, high coloration effiency, etc.) and easier processability than the inorganic and molecular counterparts.

1.2. The Brief History of CPs

The study on organic CPs for electrochromic materials was started with Shirakawa, MacDiarmid, and Heeger in 1977 [7,8]. They were awarded the Nobel Prize in chemistry in 2000 due to discovery of highly conducting iodine-doped polyacetylene [9-11]. Although iodine-doped polyacetylene has high conductivity (10^{11} S/cm), its poor stability in air prevented its commercialization for industrial applications. However, this obstacle encouraged researchers to find alternative CPs which were more stable, processable and also as conductive as polyacetylene. In the light of these studies, different electron-rich CPs consisting of polypyrrole [12], polyfuran [13], polythiophene [14, 15] and poly(3,4-ethylenedioxythiophene) (PEDOT) [16], as well as the other aromatic polymers such as polyaniline [17], poly(p-phenylenevinylene) [18] and polycarbazole [19] were developed and extensively examined as alternative CPs (Figure 1).

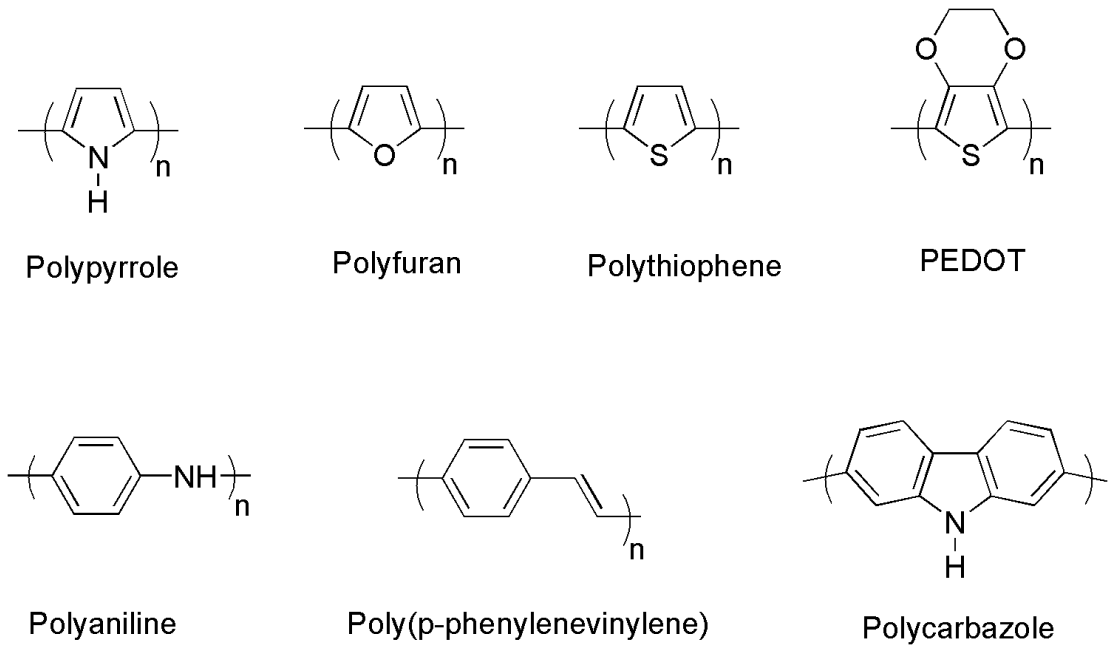

Figure 1. Some common CPs.

Although these new alternatives are not good enough to improve conductivity of polyacetylene, they show higher stability than polyacetylene. Furthermore, their structures are accessible to modify desired physical and optical properties. Hence, in the light of the tuning and structural design of these polymers [20-26] enormous efforts about electrochromism have been devoted to the design and synthesis of new polymeric electrochromics (PECs) [27-33].

1.3. Synthesis of CPs

Electrochemical and chemical polymerizations are mostly used methods for the synthesis of CPs. Besides these two techniques, plasma polymerization and copolymerization are also used for this aim.

1.3.1. Electrochemical Polymerization

Electrochemical polymerization is a simple oxidative way based on the formation of reactive radical cations from oxidation of monomer dissolved in electrolytic medium by applying proper potential to the working electrode. After the formation of reactive radical cations, there are two possible ways to form polymer. In the first way, a radical cation couples with neutral monomer and after a second oxidation, it loses two protons so it forms a neutral dimer [34]. In the second way, two radical cations couple and lose their two protons to form neutral dimer [35]. Dimer is oxidized and the possible coupling process is repeated. Also, oxidation of dimer is easier than monomer itself since the potential of dimer is lower than that of monomer. Finally, increasing chain length leads to deposition of electroactive polymer onto the working electrode. A general polymerization mechanism for heterocycles is given in Figure 2(b). Electrochemical polymerization has some advantages over other methods such as [36];

- Small amounts of monomer can be sufficient.
- Polymers can be obtained in a relatively short time period.
- In-situ analysis
- Side reactions can be eliminated by control applied potential.

- Film thickness and conductivity can be controlled by a changing applied potential, scan rate and time.

The ease with which electrons can be removed from the monomer and the stability of the resultant radical cation (Figure 2(a)) affects the efficiency of the polymerization. In fact, electron-rich monomers have the ability to lose an electron more easily than relatively electron-poor monomers. Therefore, former stabilize the resultant radical cation through resonance across the π-electron system than latter (Figure 2(a)).

During polymerization, besides α-α' coupling, some α-β coupling may also take place (Figure 2(c)). This linkage causes to chain branching with more defects and it damages the homogeneity of the polymer by producing different parts which have different electronic properties and conductivity values over polymer ring. In the case of EDOT monomer, replacing the hydrogen atoms of the 3- and 4-positions of the monomers with alkyl and alkoxy groups is one of the ways of eliminating undesired linkages (α-β, β-β).

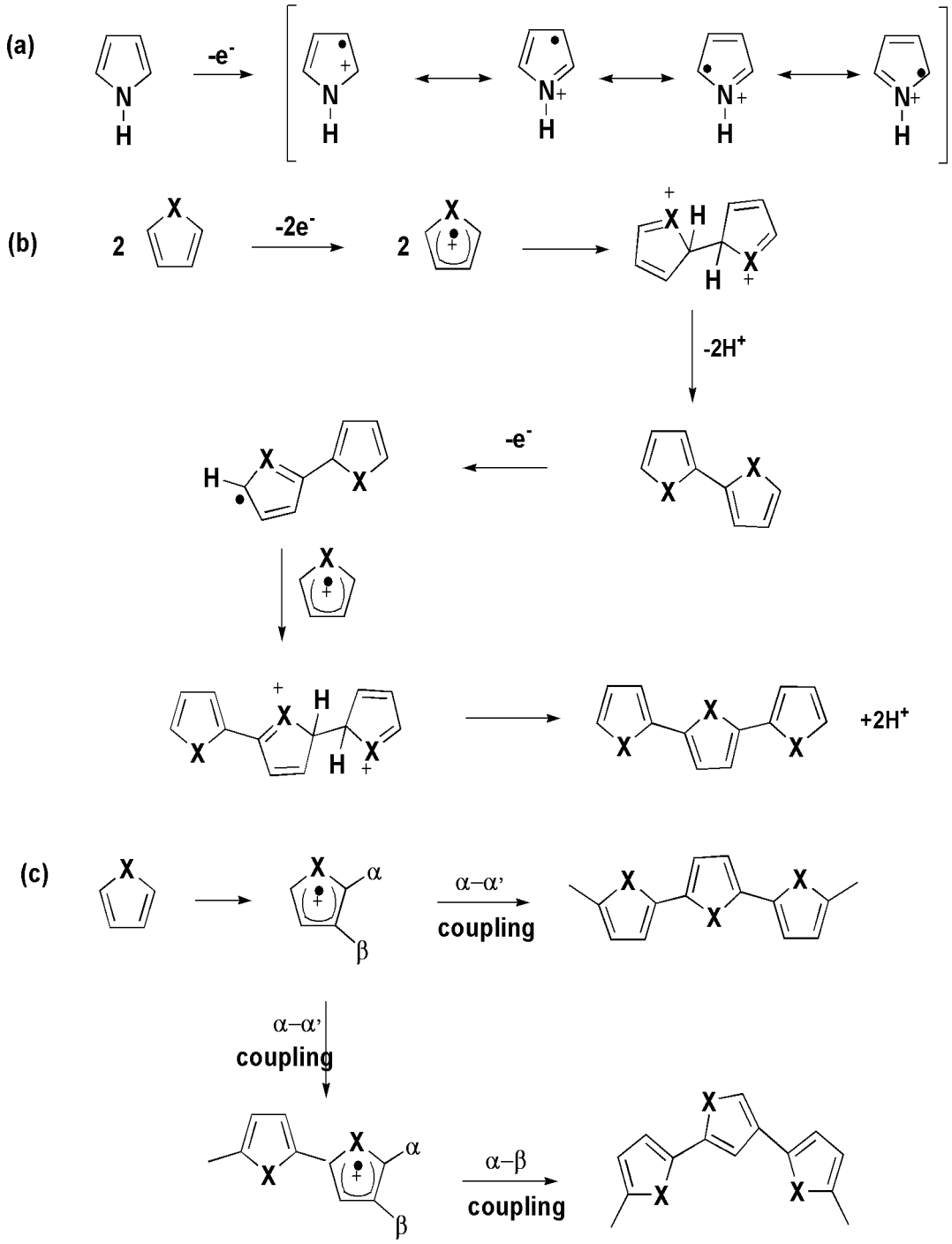

Figure 2. (a) Radical cation stability of pyrrole monomer. (b) Electropolymerization mechanism of heterocyclic monomers (X = S, O, NH). (c) Possible α-α' and α-β couplings of unsubstituted heterocylic monomers (X = S, O, NH) [37].

1.3.2. The Importance of Electrolytic Media on Electrochemical Polymerization

There are many effects which are important for electrical properties of the polymer during electrochemical polymerization such as, suitable solvent and electrolyte, monomer concentration and value of applied current. Dielectric constant of the solvent has to be high for dissociating supporting electrolyte. Moreover, it must be usable in the range of applied potential. In general, nitrile-based solvents are used. The effects of electrolytes are also crucial for polymerization because electrolytes can affect electrochemical results; hence, they must be electrochemically inactive and non-nucleophilic. Generally, lithium perchlorate, tetraalkylammonium hexafluorophosphate and tetraalkylammonium tetrafluoroborate are used in the electrochemical synthesis of CPs [38]. During the polymerization, monomer concentration is important to guarantee polymerization. Applied potential is also an effective way for reducing side reactions. For example, a low oxidation potential will avoid overoxidation of the polymers [39].

1.3.3. Chemical Polymerization

Chemical polymerization is the best technique to analyze the primary structure of CPs. Unlike the electrochemical polymerization, highly soluble polymers derived from especially substituted heterocyclic monomers can be produced by using chemical polymerization. Hence, soluble polymers make easier to analyze primary structure by using traditional techniques. For chemically synthesized CPs, catalytic Grignard reactions and oxidative methods are generally used. Actually, oxidative method has been used more than Grignard reaction because of its low cost [40]. Oxidative method is based on the formation of the polymers in their doped and conducting state by exposing the monomer to oxidative chemicals. After the formation of polymer, they are reacted with reducing agent (e.g. hydrazine or ammonia) to get neutral polymer (Figure 3 (a)). Anhydrous $FeCl_3$ is mostly used as an oxidizing agent [41]. Also, some Lewis acids can be used in chemical polymerization [42].

Catalytic Grignard reactions are commonly used for synthesizing furan, pyrrole and thiophene-based polymers [43]. The main aim of Grignard reaction is to prevent the polymer chain from undesired couplings. As illustrated, in Figure 3(b) [44], 2,5 dibromothiophene derivative is reacted with Mg metal in dry THF to generate corresponding MgBr product. Addition of metal complex catalyst such as mono (2,2-bipyridene)nickel(II) chloride initiates self-coupling reactions producing polythiophene derivatives without undesired 2,3 and 2,4 couplings [45].

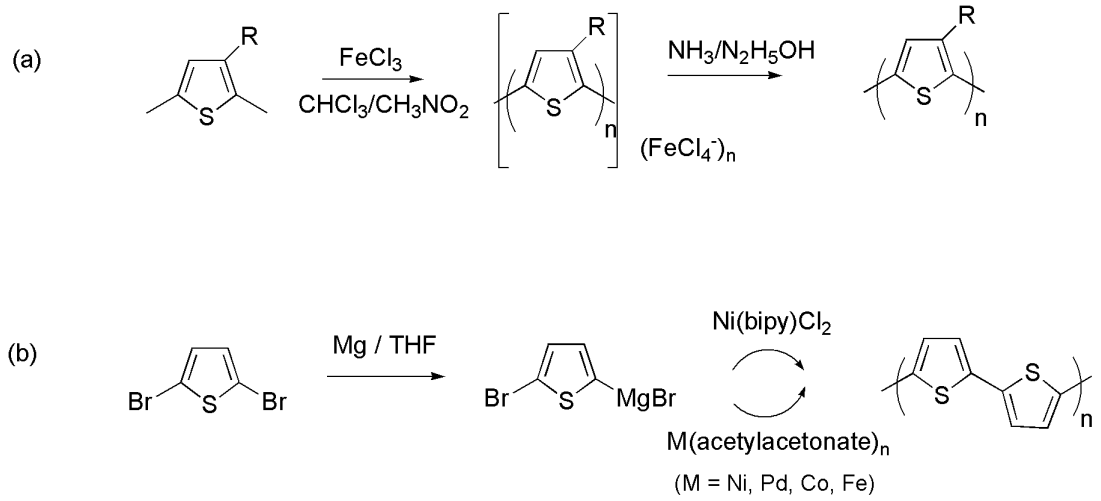

Figure 3. Chemical polymerization of thiophene via (a) oxidative method (b) catalyzed Grignard reaction.

Formation of highly soluble polymers, from especially substituted heterocyclic and aromatic monomers is the most important advantage of chemical polymerization over electrochemical polymerization. Thanks to this, some common traditional techniques can be used for characterization and analysis of these polymers. Furthermore, it is also possible to obtain the polymer in large scale by changing polymerization conditions. Although chemical polymerization methods have some advantages as stated earlier, there are some disadvantages which cause low quality polymers. Strong oxidizing agents can cause overoxidation and decomposition of the polymer [46]. In addition, polymer can precipitate in medium because Lewis acid

catalyzed polymerizations yield more rigid oxidized polymer [47] that delimitate the degree of the polymerization.

1.3.4. Band Theory

Electrical properties of a material totally depend on the movement of electrons through the structure. Conductive polymers obtain this character from charge carriers (coming from doping process) and contribution of conjugation on polymer backbones.

Band theory clarifies the electrical properties of materials with the energy differences between the highest occupied molecular orbital (HOMO) and lowest unoccupied molecular orbital (LUMO). The band gap (E_g) is determined by the differences between the conduction band (CB) and valence band (VB) [48]. For metals, E_g value is 0 eV, so only mobility of charge carriers is sufficient to achieve conduction. In semiconductors, the conduction method is different than metals because E_g values of semiconductors are between 0.5 - 3.0 eV (Figure 4). Therefore, CB must be deposited with the exciting electrons which are formed by thermally or photochemically. Doping processes (p-doping and n-doping) raise the conductivity of the material by the formation of charge carriers. On the other hand, the E_g of insulator is over 3.0 eV; therefore, they have no conductivity in normal conditions. The E_g of conductive polymer can be estimated by the onset of the π-π* transition in the ultraviolet-visible (UV-VIS) spectrum.

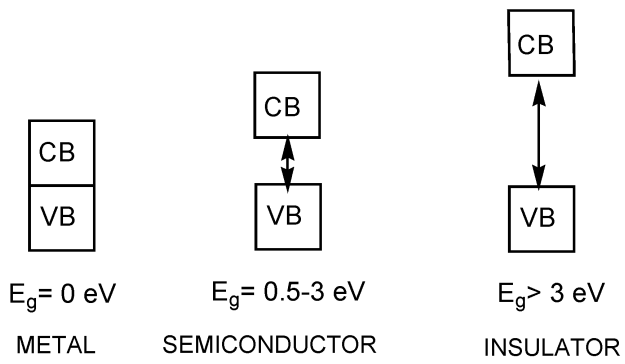

Figure 4. Band gap diagrams for metal, semiconductor and insulator materials.

1.4. The Conductivity of CPs

CPs are semiconductors. During the switching between reduction and oxidation states some defects (e.g. radicals) are formed on the polymer structure. The formation of basic conduction mechanism is related to the movement of these defects called as charge carriers. There are two types of charge carriers, namely positive (p-type) and negative (n-type) charge carriers. They are formed by oxidation or reduction of polymer. The transition of charge carriers and lowering the effective E_g enable CPs to be semiconductors.

Polarons are formed upon removal/addition of an electron from/on destabilized orbital. Further removal or addition leads to the formation of dications or dianions (bipolarons) (Figure 5).

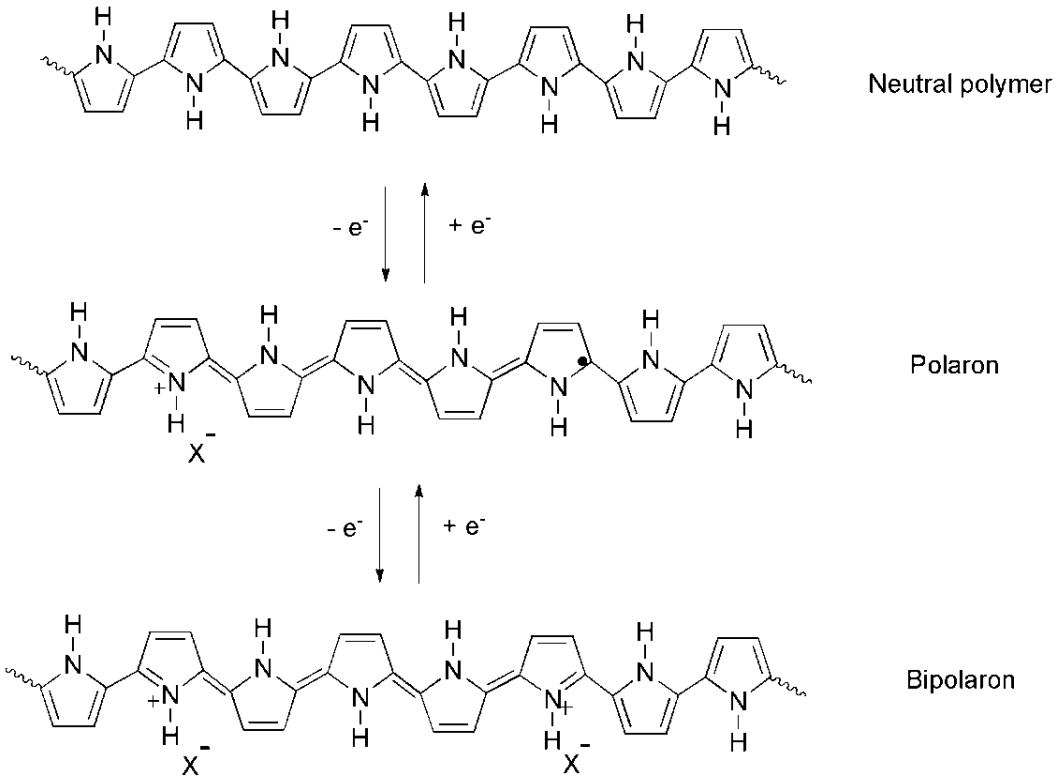

Figure 5. Formation of charge carriers in polypyrrole during oxidative doping [49].

The increasing number of bipolarons between the valence band and conduction band leads to the formation of new energy levels in this region due to the overlapping of bipolaron levels. That results in decreasing of E_g and increasing of conductivity (Figure 6).

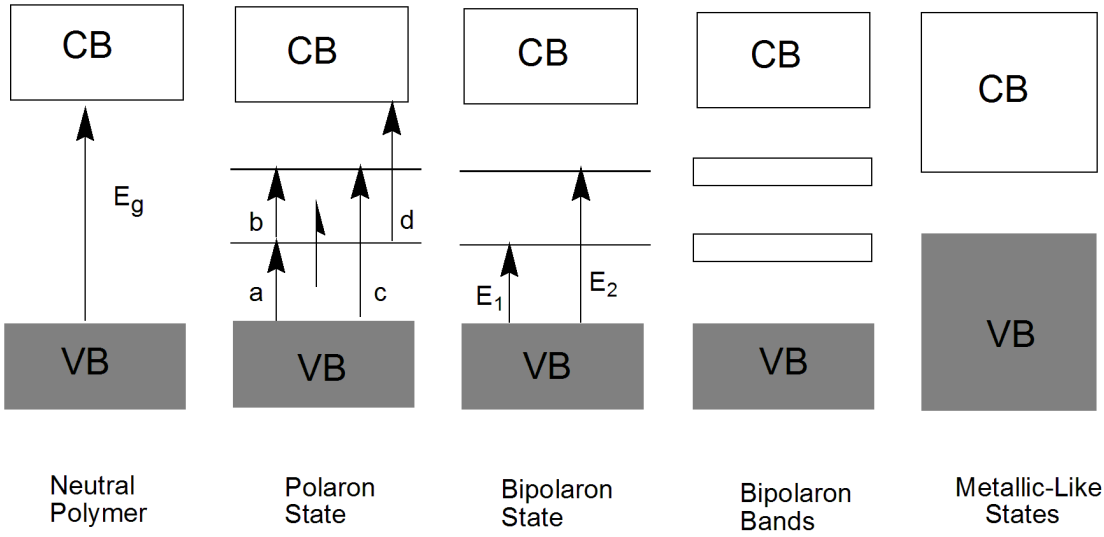

Figure 6. Increasing the conductivity of CPs in polaron state, c and d are not allowed and b is into IR region. In polaron state, E_1 observed in IR region.

1.4.1 Doping Process

The formation of radicals, cations and anions on polymer structure is called doping. There are two ways of doping, namely chemical doping and electrochemical doping. Figure 7 illustrates two types of doping.

During the chemical doping process, the control of the doping level is difficult; hence, this process may cause heterogeneous intermediate structure rather than complete doping. However, in electrochemical doping process, the degree of the doping can be controlled by adjusting potential with respect to the reference electrode [50], so it is possible to reach stable charge carriers in this way.

(A) Chemical Doping

(a) p-type doping

$$(CP)_n + 3/2\ ny(I_2) \longrightarrow [(CP)^{+y}(I_3^-)_y]_n$$

(b) n-type doping

$$(CP)_n + [Na^+(C_{10}H_8)^-]_y \longrightarrow [(CP)^{-y}(Na^+)_y]_n + C_{10}H_8$$

(B) Electrochemical Doping

(a) p-type doping

$$(CP)_n + [Li^+(BF_4^-)]_{soln} \longrightarrow [(CP)^{+y}(BF_4^-)_y]_n + Li_{elect}$$

(b) n-type doping

$$(CP)_n + Li_{elect} \longrightarrow [(CP)^{-y}(Li^+)_y]_n + [Li^+(BF_4^-)]_{soln}$$

Figure 7. (A) Chemical dopings (n-type and p-type). (B) Eectrochemical dopings (n-type and p-type) [50].

1.5 Structural Control of CPs

The structure of the monomer is very important for the CPs in determining their solubility, processability, optical and electrochemical properties. Also, CPs' properties can be tuned via structural design to get desired electrochromic properties. Hence, the design of the monomer is the first crucial step for the studies focused on CPs. After becoming one of the most popular classes of electrochromism, several aromatic and heteroaromatics CPs have been designed and produced. PANI drew to attention of scientists due to its good properties (e.g., processability and low cost) for making films that also show three distinct color states (transparent, yellow/green, blue/black) [51,52]. However, carcinogenic byproducts formed during synthesis of polyaniline samples prevent its use for industrial and academic purposes [53]. Therefore, other heterocyclic CPs gained popularity, especially polythiophene (PTh) and its derivatives are the most popular ones. Polythiophene was firstly prepared in

the beginning of the 1980's [54]. PTh has a low band gap (2.1-2.2 eV) with high HOMO level for easier oxidation, good environmental stability and also facile functionalization [55, 56]. However, PTh like other heterocylic polymers (polypyrrole, polyselenophene (PSe), etc.) suffers from β-coupling defects (Figure 2) which causes some problems for conjugation lengths, electronic and optical properties.

Blocking the β positions of the heterocycles with diverse substituents is the mostly used procedure to obtain main chain perfections and enhance electronic and optical properties [37]. For example, methyl substituted thiophene derivatives (Figure 8) exhibits higher conductivity and higher conjugation length than the parent PTh [57]. Moreover, methyl substituents decrease the oxidational potential.

Similarly, when alkoxy-groups were added to thiophene ring as substituent, the oxidation potential of the system decreases due to electron donation effect[58]. However, 3,4-disubstituted thiophene polymers show higher oxidational potentials and lower band gaps, as well as, lower conductivities, compared to their monosubstituted analogues [59].

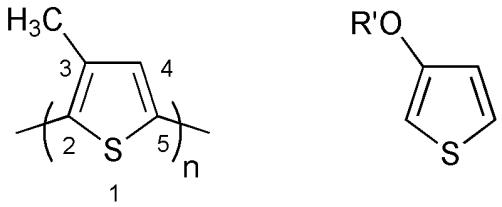

Figure 8. Structure of Th ring with alkyl and alkoxy substituents.

1.6 Poly(3,4-ethylenedioxythiophene) (PEDOT)

To eliminate the problems which restrict the electrosynthesis and electronic properties of first generation of CPs, poly(3,4-ethylenedioxythiophene) (PEDOT) (in group of second generation CPs) was produced after polymerization of 3,4-dimethoxythiophene (EDOT) (Figure 9). The cyclic ethylenedioxy bridge which block the β-positions not only comfort steric strain but also increase the electron

density of the heterocyclic PTh ring. It was the first promising candidate to overcome solubility problem of CPs in common organic solvents [16]. However, this ambition was not realized due to the insolubility of PEDOT in common organic solvents. On the other hand, it has lower oxidation potential than PTh, which leads to more stable doped state [60]. Moreover, it reduced the band gap, resulting in more transmissive doped state and more absorptive neutral state.

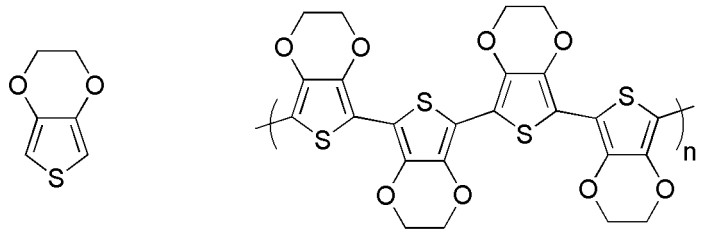

Figure 9. Structure of EDOT and PEDOT.

After the polymerization of EDOT, many studies about synthesizing its derivatives and changing the original EDOT structure have been reported. In this respect, Reynolds and his coworkers investigated the electrical and optical properties of 3,4-alkylenedioxythiophene derivatives [28]. Additionally, in this manner pyrrole heterocycles and its derivatives have been produced and polymerized in electrochemical way [61]. Furthermore, for decreasing monomer oxidation potential, multi-ring and extended monomer conjugation have been reported (Figure 10) [26,62,63] since their longer conjugation lengths leads to high valence band energy and more stable radical cation during electrochemical oxidation. Also, these heterocyclic structures can be used in donor-acceptor-donor (DAD) systems as donor units.

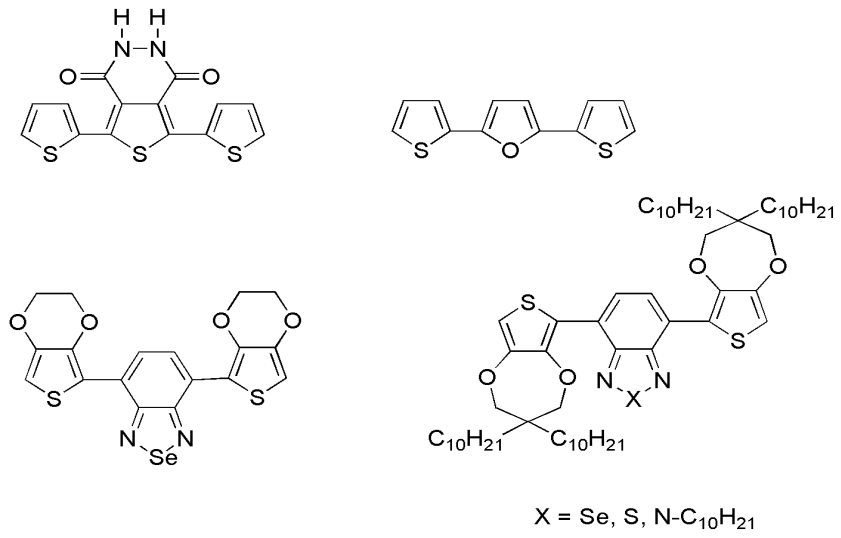

Figure 10. Some extended conjugation heterocycle-based structures suitable for electrochemical polymerization.

1.7 Poly(3,4-propylenedioxythiophene) (PProDOT)

The solubility problem of PEDOT forces scientists to develop new monomer structures. In the advantage of synthetic flexibility of PEDOT, Reynolds and his coworkers have been studied with various alkylenedioxythiophenes bearing different ring size, number and placement of substituents on the ring [64]. Disubstituted poly(3,4-propylenedioxythiophene)s (PProDOTs) make useful to form regiosymmetric polymers and lead to solubility in common organic solvents [31]. Additionaly, the propylenedioxy ring prevents the conjugation along the polymer chain structure from the alkyl chains due to forming space to separate alkyl chains from the polymer backbone. In fact, dimethyl substituted propylenedioxythiophene, PProDOT-C_1, (Figure 11) shows the best values in the alkylenedioxythiophene family. It has a contrast ratio of 78% at 585 nm and it switches in 0.3 s [65]. In the literature, ProDOT-Bz_2 exhibited the highest contrast ratio (89%) among the polymers synthesized electrochemically [66]. Although all substituents gained better electrochromic properties to parent sutructure, only butyl and longer ones provide solubility to parent structure in common organic solvents.

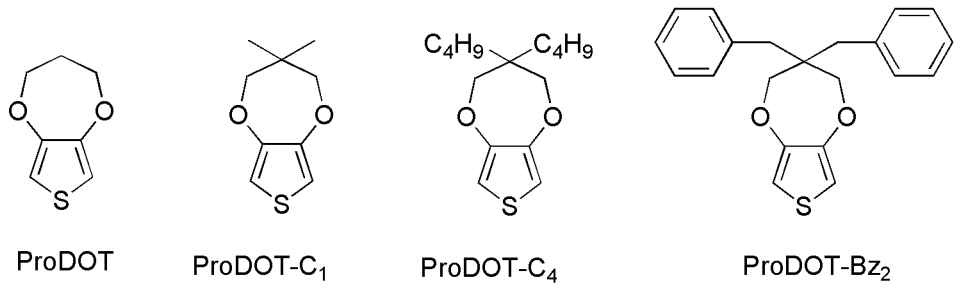

Figure 11. Structure of ProDOT and its derivatives.

1.8 Selenophene Based Polymers

It is well-known that different heteroatoms (e.g. S, O, N) in similar systems (thiophene, pyrrole, furan, etc.) could affect the ease of polymerization and the properties of the corresponding polymers. For example, under the polyelectrochromics umbrella, PThs and their derivatives, especially alkylenedioxythiophenes (XDOTs) [67], are one of the most promising materials due to their optical and electronic properties. However, the similarity between S and Se rings, and considering that Se analogues of tetrathiafulvalene (TTF), such as tetramethyltetraselenafulvalene (TMTSF), and biethylenethiaselenophene (BETS), have been shown to be even better organic superconductors than TTF derivatives [68], it is suprising that very little is known about polyselenophene [61,69]. In fact, XDOTs' properties can be tuned by the replacement of the S atom by the Se atom. Moreover, PSe can become a crucial member of the CP family since Se atom has less electronegativity, more metallic character, large atomic size and more polarizability compared to S atom. Intermolecular interactions between Se atoms lead to a better interchain charge transfer for the PSe (Figure 12). Moreover, the size of the Se atom is larger than S atom, which enables PSe to accommodate more charge during oxidative doping [32].

However, even in the presence of these possible advantages over PTh, PSe has not attracted as much attention as PTh, probably because of the difficulties in the synthesis. In addition, previous reports [61,69] showed that the conductivity of oxidized PSe range from 10^{-4} to 10^{-1} S cm^{-1}, which is actually lower than PTh (up to

1000 S cm^{-1}) [27]. This may be another reason why PSe remained unremarkable. However, Bendikov and his coworkers reported their computational results about PSe, indicating that there is no clear reason for their lower conductivies as compared to PTh. Therefore, they expect the conductivity of PSe as same as or even higher than that of PTh [70].

Figure 12. Structure of PSe and 3,4-dimethoxyselenophene.

Furthermore, they recently [71] developed a new rational synthetic route for 3,4-ethylenedioxyselenopehene (EDOS) (Figure 13) and reported a low band gap (1.4 eV) polymer film (PEDOS) exhibiting electrochromic behavior with high contrast ratio and coloration efficiency, long term stability and high conductivity (3-7 S/cm). The absence of absorption between 400 nm and 500 nm resulted in a pure blue color when compared to PEDOT, which makes it a promising candidate for electrochromic devices. Unfortunately, the lack of solubility of PEDOS and its alkyl substituted derivatives (PEDOS-C_n, n: 2, 4, 6, 8 and 12) [72, 73] hampered their use in opto-electronic devices.

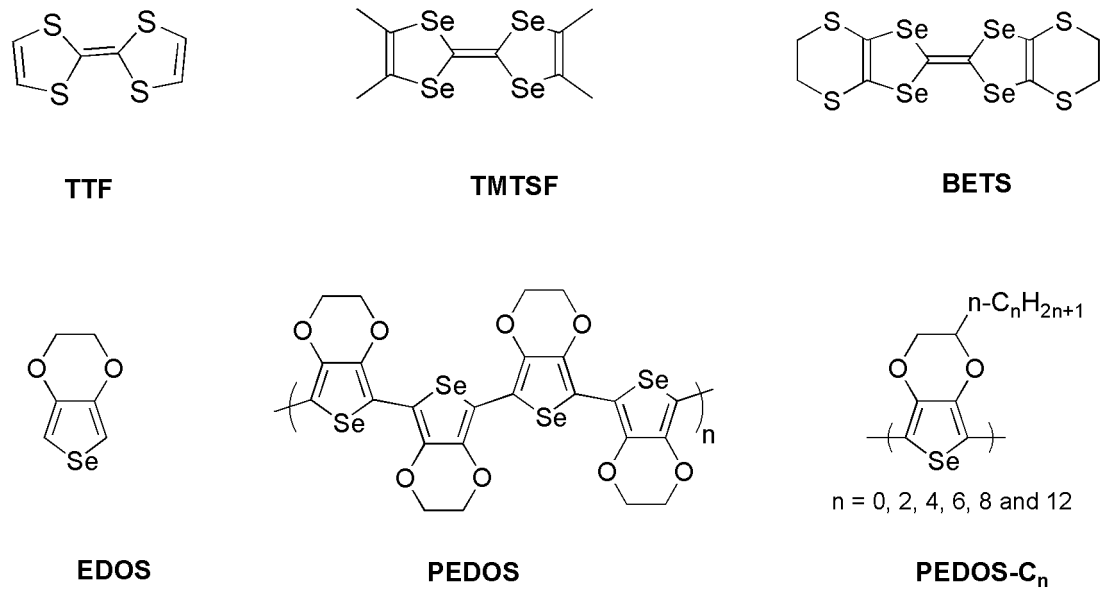

Figure 13. Structures of some tetraselenafulvalene and EDOS derivatives

1.9. Characterization of CPs

The characterization of electroactive polymers is more difficult than that of the conventional polymers due to the solubility problem in common organic solvents. Hence, lots of electroanalytical techniques can be applied for characterization of CPs. Among them, cyclic voltammetry (CV) is most widely used for studying the redox behavior of conductive monomers and polymers. Moreover, CV shows that the stability of the polymer after multiple redox cycles. Nuclear magnetic resonance (NMR) is used for soluble monomer and polymers to understand their structure, chain and molecular orientation. To analyze the molecular weight of the polymer, gel permeation chromatography (GPC) can be used. Fourier transform infrared spectrometry (FTIR) can be used to analyze functional groups and dopant ions in the polymer chain. To analyze the band gap of the polymer and its spectroelectrochemical behaviors, UV-vis spectrometers can be used. The colors or tones of a polymer can be described with colorimeter for quantitative and objective results.

1.10 Electrochromic Properties

1.10.1 Contrast Ratio

Contrast ratio (Δ%T) is defined as the change in percent transmittance between undoped (neutral) and doped (bleached) states. The contrast ratio is calculated at a specified wavelength where the polymers have the highest optical contrast [74]. The reported highest Δ%T (89%) belongs to PProDOT-Bz_2 [66] and PEDOS-C_6 [73]. Contrast ratio value can be calculated by the differences between percent tranmittance of polymer at oxidized state (T_{ox}) and transmittance of reduced state (T_{red}) (Equation 1-1).

$$\Delta\%T = T_{ox} - T_{red} \qquad (1\text{-}1)$$

1.10.2. Coloration Efficiency

The simple definition of coloration efficiency (CE) is that the efficiency of the color changes that occur in response to applied charge. The ideal polyelectrochromic would show a high transmittance change by applying low charge to get large CEs. CPs show higher CE values than inorganic counterparts in the visible region. The coloration efficiency is calculated by the Equation 1.2 where $\Delta OD = \log [T_{ox}/T_{red}]$ [83,84]. ΔOD is the change in optical density at a specific wavelength, Q_d is injected or ejected charge as a function of electrode area.

$$CE = \Delta OD (\lambda) / Q_d \qquad (1\text{-}2)$$

1.10.3 Switching Time

The time which was needed for the optical transitions between oxidized and reduced state of CPs is called switching time (t_s). It can be affected from some factors such as polymer morphology, ions activity in electroactive sites and conductivity of electrolytes. All applications reguire differents t_s; for example, it has to be very small (miliseconds) for electrochromic displays; however, minutes are sufficient for window~~s~~ coatings to light or heat control.

1.11. Applications of CPs

The use of organic materials as electrochromic materials, in particular CPs, offers several advantages over inorganic solids including low cost, easy processing,

compatibility and tunable intrinsic properties (e.g., electronic, optical, conductivity and stability). Due to these properties, they became candidates in a wide range of application areas. These applications can be separated into three main groups. The first group includes neutral CPs which can be used for semiconducting applications such as transistors [75] and active material in light emitting devices [76]. The doped and conducting states of CPs, second group, can be used in capacitors and antistatic caotings in photographic film [16]. The third group consists of CPs having the reversible switching ability between doped and undoped states. During the switching process, color, conductivity and volume may change. This group can be used in pertinent applications including battery electrodes [77], drug delivery [78], mechanical actuators [79] and electrochromics [2]. Moreover, CPs can be used in some military applications where both dynamic visible and infrared absorbance-reflactance changes are desired. Recently, soluble CPs can be used in future applications relying on printable conducting inks for displays and inexpensive circuit boards.

1.12. Aim of This Study

Although PEDOS and its derivatives have good electrochromic properties, there must be alternative polymers which are not only soluble but also having good electrochromic properties. The best way to overcome its solubility problem could be the replacement of ethylenedioxy bridge in EDOS by a long alkyl substituted propylenedioxy bridge. It can be expected that 3,4-propylenedioxyselenophene (ProDOS) (Figure 14) units would result in low oxidational potential, high transmittance contrast ratio, high transparency when oxidized and subsecond switching times between redox states due to its electron rich nature like its sulphur analogue, 3,4-propylenedioxythiophene (ProDOT) [64,80]. It is well-known that the presence of alkyl chains attached to ProDOT units would also increase the solubility and the processability of the corresponding system [67,81]. Furthermore, alkyl substituted polyselenophenes (PEDOS-C_n) derivatives are regioirregular and atactic polymers due to the lack of symmetry in the monomers that can be easily

surmounted by the dialkylated ProDOS units which yield regioregular and isotactic polymer without a regioirregular polymerization.

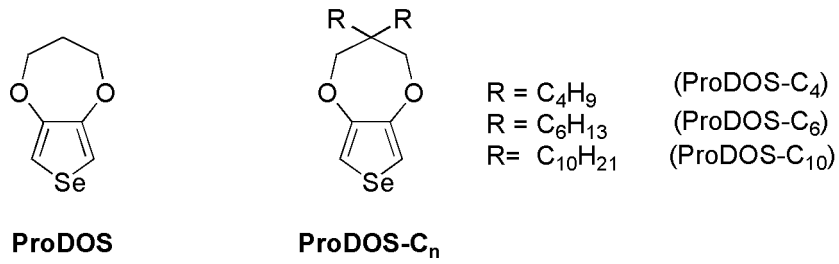

Figure 14. Structure of ProDOS and ProDOS-C_n (n = 4, 6, 10).

Recently, there have been great efforts about CPs due to these unique electrical and optical properties. Although, all novel polymers showed well development about electrochromic properties, only a few of them get soluble and processable. Hence, synthesizing soluble polymers which have good electrochromic properties must be the main aim of scientists who deal with electrochromism. Herein, the aim of the study is to synthesize regioregular and soluble electrochromic polymers based on ProDOS units, namely 3,3-dibutyl-3,4-dihydro-2H-selenopheno[3,4-b][1,4]dioxephine (PProDOS-C_4), 3,3-dihexyl-3,4-dihydro-2H-selenopheno[3,4-b][1,4]dioxephine (PProDOS-C_6), 3,3-didecyl-3,4-dihydro-2H-selenopheno[3,4-b][1,4]dioxephine (PProDOS-C_{10}) for the first time. Also, their electrochemical and optical properties will be studied and furthermore the related polymers have been discussed in comparison with their Th analogues.

CHAPTER 2

EXPERIMENTAL

2.1 Materials

All chemicals were purchased from Aldrich Chemical and used as received except for lithium aluminum hydride (Acros Chemical). For electrochemical experiments, tetrabutylammonium hexafluoraphosphate (TBAH) dissolved in freshly distilled acetonitrile (ACN) and dichloromethane (DCM) (over CaH_2 under N_2 or Ar atm) solvents were used as electrolyte solutions.

2.2. Cyclic Voltammetry (CV)

Cyclic voltmmetry (CV) is one of the widely used electroanalytical techniques for the synthesis and characterization of CPs because its usage can be simple and well-rounded. This method monitors the resulting current flow between working (WE) and counter electrodes as a function of the applied potential.

CPs are deposited onto the WE and it can be observed by the help of the increasing anodic and cathodic peak currents of redox couple. Also, polymer redox behaviours are characterized by the magnitutes of its peak potentials.

For the CV studies, a Gamry PCI4/300 and Reference 600 potentiostat-galvanostat were used. Potentiostats can eliminate voltage drop problem by keeping constant to the voltage difference between the WE and the reference electrode (RE) constant. A standart three-electrode setup which contains WE (a platinum disk, 0.02 cm^2), counter electrode (platinum wire) and RE (Ag/AgCl) connected to a potentiostat.

2.3. Spectroelectrochemistry

Spectroelectrochemistry reveals the changes in electronic transitions of CPs during the redox switching. Also spectroelectrochemistry gives information about the E_g values and intraband states that formed upon doping of the materials.

Optical measurments were carried out with a Hewlett-Packard 8453A diode array UV-vis and SPECORD S 600 spectrometers using a well-considered designed three-electrode cell to allow potential application as monitoring the absorbtion spectra. An indium tin oxide (ITO, Delta Tech. 8-12 Ω, 0.7 cm x 5 cm) was used as a WE, and a Pt wire as a counter electrode and a Ag wire as a pseudo-reference electrode. All electrodes were connected to potentiostat.

2.4. Kinetic Studies

Percent transmittance differences (Δ%T), coloration efficiency (CE) and switching time (t_s) of the material can be analyzed with kinetic studies. Also this method gives information about the capacity of the polymer to be used as electrochromic materials in advanced applications. Kinetic studies were carried out with a Hewlett-Packard 8453A diode array UV-vis and SPECORD S 600 spectrometers. An ITO as a WE, a Pt wire as a counter electrode and a Ag wire as a pseudo-reference electrode were used in UV-vis electrolysis cuvette.

2.5. Spectroscopic Measurements

2.5.1. UV Measurements

UV measurements were carried out with a Hewlett-Packard 8453A diode array UV-vis and SPECORD S 600 spectrometers using a well-considered designed three-electrode cell to allow potential application as monitoring the absorbtion spectra.

2.5.2. Nuclear Magnetic Resonance (NMR)

^{1}H NMR and ^{13}C NMR spectra were recorded on a Bruker Spectrospin Avance DPX-400 Spectrometer at 400 MHz and chemical shifts were given relative to tetramethylsilane as the internal standard.

2.5.3. Fourier Transfor Infrared Spectrometer (FTIR)

FTIR spectra were recorded on Nicolet 510 FT-IR with an attenuated total reflectance (ATR).

2.6. Colorimetric Measurements

Calorimetric measurments were achieved utilizing Specord S 600 (standart illuminator D65, field of with 10°observer), color space were given by (CIE) Luminance (L), hue (a) and intensity (b). Platinum cobalt DIN ISO 621, iodine DIN EN 1557 and Gardner DIN ISO 6430 are the references of colorimetric measruments.

2.7. Mass Spectrometer

High resolution mass spectrometry analysis of the monomers was done via Water, Synapt HRMS instrument. GPC analysis of the polymers was carried out with Polymer Laboratories PL-GPC 220 instrument.

2.8. Synthesis of Monomers

2.8.1. A General Route for Synthesis of 2,2-dialkyl Malonic Acid Diethylester

A 500 mL two-necked flask equipped with reflux condenser was filled with dry ethanol (160 mL). Sodium metal (0.2 mol, 3.25 equivalents) was added and stirred to resolve all of the sodium. After slow addition of diethyl malonate (0.062 mol, 1 eq.), the reaction mixture was heated to reflux. When it starts to reflux, 1-bromoalkyl (0.23 mol, 3.65 eq.) in 30 mL ethanol was added slowly and refluxed 4 days. After removing the ethanol, cold water was added and extracted with cold ether. Organic layer was dried with anhydrous $MgSO_4$ and the solvent was removed under reduced pressure (Figure 15).

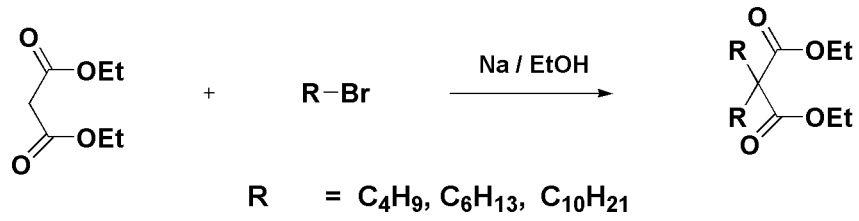

Figure 15. Synthesis of 2,2-dialkyl Malonic Acid Diethylester.

2.8.1.1. 2,2-Dibutyl Malonic Acid Diethylester

Colorless liquid. Yield: 70%. ^{1}H NMR (400 MHz, $CDCl_3$): δ (ppm) 4.20 (q, 4H), 1.90 (m, 4H), 1.43-1.00 (m, 8H), 0.89 (t, 6H).

2.8.1.2. 2,2-Dihexyl Malonic Acid Diethylester

Colorless liquid. Yield: 71%. ^{1}H NMR (400 MHz, $CDCl_3$): δ 4.18 (q, 4H), 1.89 (m, 4H), 1.41-1.00 (m, 16H), 0.88 (t, 6H).

2.8.1.3. 2,2-Didecyl Malonic Acid Diethylester

Colorless liquid. Yield: 80%. ^{1}H NMR (400 MHz, $CDCl_3$): δ 4.15 (q, 4H), 1.83 (m, 4H), 1.38-1.00 (m, 32H), 0.86 (t, 6H).

2.8.2. A Genetal Route for Synthesis of 2,2-Dialkyl-1,3-propanediol

$LiAlH_4$ (72 mmol, 1.79 eq.) was placed in a 250 mL two-necked flask equipped with reflux condenser under N_2 atmosphere. Before the addition of solvent, N_2 should be sweep the medium. Then, 100 mL dry THF was added to the reaction flask. During the process, the reaction was purged with N_2 continued. Diethyl-2,2-dialkylmalonate (40 mmol, 1 eq.) was added with a syringe. The reaction was stopped after one day. 0.1 M H_2SO_4 solution was added with a syringe very slowly, drop by drop. A salty solution was observed. Then solution was extracted with diethyl ether (Figure16).

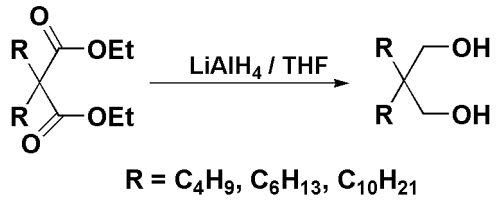

Figure 16. Synthesis of 2,2-Dialkyl-1,3-propanediol.

2.8.2.1. 2,2-Dibutyl-1,3-propanediol

Colorless liquid. Yield: 78 % ^{1}H NMR (400 MHz, $CDCl_3$): δ 3.63 (s, 4H), 2.14 (s, br, 2H), 1.43-1.00 (m, 8H), 0.89 (t, 6H).

2.8.2.2. 2,2-Dihexyl-1,3-propanediol

Colorless liquid. Yield: 80%^{1}H NMR (400 MHz, $CDCl_3$): δ 3.60 (s, 4H), 2.12 (s, br, 2H), 1.41-1.00 (m, 16H), 0.88 (t, 6H).

2.8.2.3. 2,2-Didecyl-1,3-propanediol

Colorless liquid. Yield: 80%^{1}H NMR (400 MHz, $CDCl_3$): δ 3.56 (s, 4H), 2.08 (s, br, 2H), 1.38-1.00 (m, 32H), 0.86 (t, 6H).

2.8.3. Synthesis of 3,4-Dimethoxyselenophene

Selenium powder was placed in a 25 mL flask. Then, SO_2Cl_2 (20 mmol, 1 eq.) was added to it at 10-20° C. After 20 min., 10 mL hexane was added to mixture and the reaction mixture was stirred for 3 h at room temperature (rt). A clear brown solution of $SeCl_2$ was formed. A freshly produced $SeCl_2$ in hexane was added to the stirred mixture of 2,3-dimethoxy-1,3-butadiene (17.5 mmol, 0.875 eq.) and CH_3COONa (50 mmol, 2.5 eq.) in hexane (120 mL) at -78° C (dry ice/acetone bath) under an inert atmosphere (Figure 17). A yellowish solution was formed after mixing two solutions. Then, the yellowish solution was stirred for 1 h at -78° C. After 1 h, the resulting reaction solution was removed from bath and was brought to rt over 1 h and further stirred for 4 h. The mixture was chromatographed on silica gel by eluting with methylene chloride: hexane (1:1, v/v) to give the product as yellow viscous liquid in 32% yield. ^{1}H NMR (400 MHz, $CDCl_3$): δ 6.55 (s, 2H), 3.85 (s, 6H). ^{13}C NMR (62.5 MHz, $CDCl_3$): δ 148.9, 96.0, 57.0.

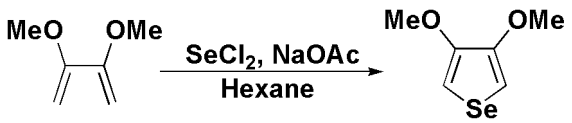

Figure 17. Synthesis of 3,4-dimethoxyselenophene.

2.8.4. A General Route for Synthesis of 3,3-Dialkyl-3,4-dihydro-2H-selenopheno[3,4-b][1,4]dioxepines

To an argon degassed solution of 3,4-dimethoxyselenophene (0.806 mmol, 1 eq.), 2,2-dihexylpropane-1,3-diol (1.613 mmol, 2 eq.) and p-toluenesulfonic acid (PTSA) (0.00806 mmol, 0.1 eq.) were mixed in dry toluene (20 mL) and the mixture was heated under reflux during 24 h (Figure 18). After cooling to rt, the solvent was removed under reduced pressure. The crude mixture was chromatographed on silica gel by eluting with DCM: hexane (1:4, v/v) to give ProDOS-C_n.

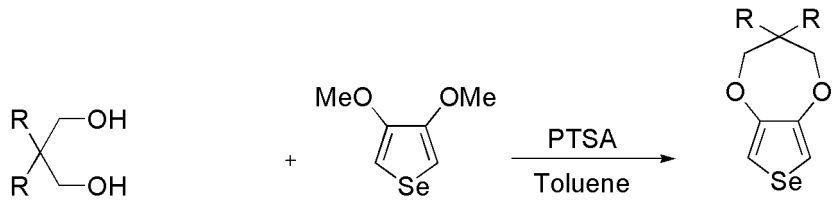

ProDOS-C_4 (R = C_4H_9), ProDOS-C_6 (R = C_6H_{13}), ProDOS-C_{10} (R = $C_{10}H_{21}$)

Figure 18. Synthesis of ProDOS-C_n (n = 4, 6, 10).

2.8.4.1. ProDOS-C_4

Clear yellowish liquid. Yield: 53%. ^{1}H NMR (400 MHz, $CDCl_3$, δ): 6.91 (s, 2H, Ar H), 3.84 (s, 4H), 1.37-1.27 (m, 12H), 0.92 (t, 6H). ^{13}C NMR (100 MHz, $CDCl_3$, δ): 150.81, 107.04, 43.77, 31.94, 25.04, 23.55, 14.05. FTIR (ATR cm^{-1}): 3109, 2956, 2929, 2861, 1477, 1365, 1151, 1113, 1021, 763, 661. UV-vis λ_{max}: 268 nm.

2.8.4.2. ProDOS-C_6

Clear yellowish liquid. Yield: 55%. ^{1}H NMR (400 MHz, $CDCl_3$, δ): 6.90 (s, 2H, Ar H), 3.83 (s, 4H), 1.32-1.28 (m, 20H), 0.89 (t, 6H). ^{13}C NMR (100 MHz, $CDCl_3$, δ): 149.82, 106.52, 42.84, 30.86, 30.72, 29.13, 28.69, 21.78, 13.04. FTIR (ATR cm^{-1}): 3109, 2956, 2929, 2857, 1477, 1368, 1151, 1110, 1018, 766, 661. UV-vis λ_{max}: 267 nm.

2.8.4.3. ProDOS-C_{10}

Clear yellowish liquid. Yield: 55%. ^{1}H NMR (400 MHz, $CDCl_3$, δ): 6.81 (s, 2H, Ar H), 3.75 (s, 4H), 1.25-1.12 (m, 36H), 0.81 (t, 6H). ^{13}C NMR (100 MHz, $CDCl_3$, δ): 149.78, 105.99, 42.82, 30.88, 30.76, 29.45, 28.61, 28.58, 28.51, 28.31, 21.79, 21.66, 13.10. FTIR (ATR): 2920, 2853, 1467, 1364, 1148, 1107, 1022, 981, 762, 720, 662, 618 cm^{-1}. UV-VIS λ_{max}: 268 nm.

2.8.5. A General Route for Synthesis of 3,3-Dialkyl-3,4-dihydro-2H-thieno[3,4-b][1,4]dioxepines

To an argon degassed solution of 3,4-dimethoxythiophene (0.68 mmol, 1 eq.); 2,2-dihexylpropane-1,3-diol (1.36 mmol, 2 eq.) and p-toluenesulfonic acid (PTSA) (0.068 mmol, 0.1 eq.) were mixed in dry toluene (20 mL) and the mixture was heated under reflux during 24 h (Figure 19). After cooling to rt, the solvent was removed under reduced pressure. The crude mixture was chromatographed on silica gel by eluting with DCM: hexane (1:4, v/v) to give ProDOT-C_n.

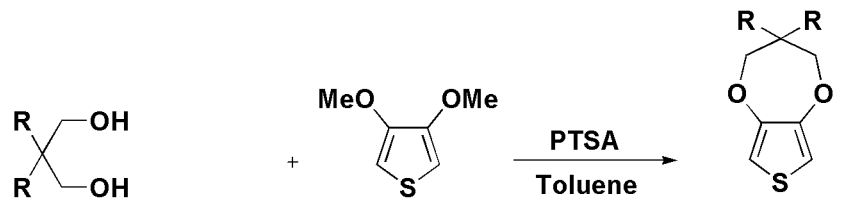

ProDOT-C_4 (R = C_4H_9), ProDOT-C_6 (R = C_6H_{13}), ProDOT-C_{10} (R = $C_{10}H_{21}$)

Figure 19. Synthesis of ProDOT-C_n (n = 4, 6, 10).

2.8.4.1. ProDOT-C_4

Clear yellowish liquid. Yield: 60%. ^{1}H NMR (400 MHz, $CDCl_3$, δ): 6.40 (s, 2H, Ar H), 3.85 (s, 4H), 1.38-1.26 (m, 12H), 0.90 (t, 6H). ^{13}C NMR (100 MHz, $CDCl_3$, δ): 149.74, 104.64, 43.67, 31.94, 29.67, 25.04, 14.11. FTIR (ATR, cm^{-1}): 3340, 2950, 2927, 2853, 1458, 1375, 1210, 1150, 1029, 889, 763, 665.

2.8.4.2. ProDOT-C_6

Clear yellowish liquid. Yield: 62%. ^{1}H NMR (400 MHz, $CDCl_3$, δ): 6.41 (s, 2H, Ar H), 3.83 (s, 4H), 1.31-1.28 (m, 20H), 0.91 (t, 6H). ^{13}C NMR (100 MHz, $CDCl_3$, δ): 149.74, 104.63, 43.75, 31.89, 31.73, 30.14, 22.78, 22.64, 14.05. FTIR (ATR, cm^{-1}): 3342, 2958, 2928, 2860, 1468, 1377, 1212, 1152, 1031, 888, 753, 662.

2.8.4.3. ProDOT-C_{10}

Clear yellowish liquid. Yield: 59%. ^{1}H NMR (400 MHz, $CDCl_3$, δ): 645 (s, 2H, Ar H), 3.75 (s, 4H), 1.25-1.12 (m, 36H), 0.80 (t, 6H). ^{13}C NMR (100 MHz, $CDCl_3$, δ): 149.32, 104.21, 48.25, 34.27, 31.21, 30.09, 29.23, 28.95, 28.67, 27.56, 24.88, 22.41, 13.71. FTIR (ATR, cm^{-1}): 3113, 2922, 2849, 1571, 1486, 1459, 1374, 1183, 1117, 1018, 847, 761, 715, 669.

2.9. Electrochemical Polymerization

For the electrochemical polymerization of monomers (ProDOS-C_4, ProDOS-C_6, ProDOS-C_{10}) concentrations were between 1.0 x 10^{-2} and 3.5 x 10^{-2}. In all electrochemical polymerization experiment ACN/DCM mixture (95/5, v/v) was used as a solvent. DCM dissolves the monomer and supporting electrolyte, and ACN prevents dissolution of the polymers. TBAH was used as a supporting electrolyte in all experiments. Three-electrode system was used in CV because of measurement of current and potential at the same time.

CHAPTER 3

RESULTS AND DISCUSSION

3.1. Electrochemical Properties of Monomers

3.1.1. Cyclic Voltammograms of Monomers

Electrochemical behavior of ProDOS-C_n (n = 4, 6, 10) monomers were investigated in 0.1 M TBAH/DCM solution utilizing CV. The voltammogram of ProDOS-C_4 exhibited irreversible oxidation peak at 1.44 V vs. Ag/AgCl during anodic scan. Like ProDOS-C_4, the oxidation potentials of ProDOS-C_6 and ProDOS-C_{10} were observed at 1.36 V and 1.39 V vs. Ag/AgCl respectively (Figure 20). These oxidation potentials are lower than those of ProDOT-C_n analogues (1.53 V for ProDOT-C_4, 1.52 V for ProDOT-C_6 and 1.55 V for ProDOT-C_{10} vs. Ag/AgCl) (Figure 20). Therefore, it can be concluded that ProDOS-C_n has more electron rich nature than ProDOT-C_n, as expected when replacing the S atom by the Se atom in the similar system, which may be attributed to the lower electronegativity of Se than S. However, when compared to the first monomer oxidation potential of EDOS (1.22 V) [65], ProDOS-C_n has higher oxidational potential due to the larger alkylenedioxy ring size which results in a decrease in the electron donating abilities of oxygen atoms. In fact, compared to first oxidation peaks of ProDOS-C_n monomers, ProDOS-C_6 has the lowest oxidational potential. Also, the same trend can be seen in ProDOT-C_6 in ProDOT-C_n (n = 4, 6, 10) monomers. Therefore, we can say that hexyl-substituents are more effective than other alkyl-substituents to decrease monomer oxidation potential.

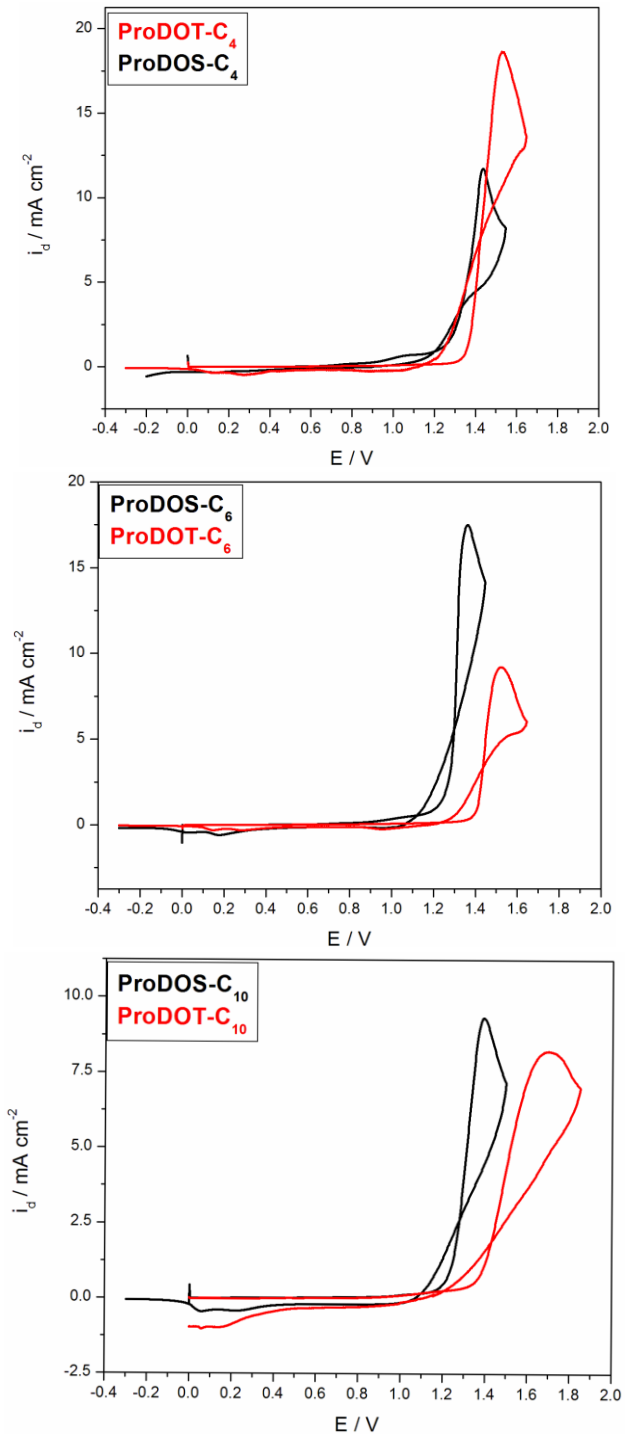

Figure 20. Cyclic voltammograms of ProDOS-C_n and ProDOT-C_n (n = 4, 6, 10) in 0.1 M of TBAH dissolved in DCM at 100 mV/s vs. Ag/AgCl. The monomer concentrations; 1 x10^{-2} M ProDOS-C_4; 1.5 x10^{-2} M ProDOT-C_4; 1.8 x10^{-2} M ProDOS-C_6; 1.3 x10^{-2} M ProDOT-C_6; 3.5 x10^{-2} M ProDOS-C_{10}; 3.3 x10^{-2} M ProDOT-C_{10}.

3.1.2. Electropolymerization of Monomers

The polymer films deposited on WE during the electropolymerization of ProDOS-C_n to get PProDOS-C_n were highly soluble in DCM, so the electropolymerization of monomers were performed in a mixture of DCM and ACN (5/95, v/v) containing 0.1 M TBAH as supporting electrolyte via potential cycling. In the electropolymerization processes, new reversible redox couples appeared at about 0.22 V for ProDOS-C_4, 0.19 V for ProDOS-C_6, 0.28 V for ProDOS-C_{10} during repetitive anodic scans (Figure 21). Also, during the repetitive anodic scans the current intensities of these new reversible redox couples were found to increase. The increase of the current intensities indicates the formation of an electroactive PProDOS-C_n polymer film on the working electrode with increasing polymer film thickness. Also, the electropolymerization of the ProDOT-C_n to get PProDOT-C_n was investigated in the same medium of PProDOS-C_n. Like ProDOS-C_n analogues, these monomers also easily polymerized, and during dynamic electropolymerization, new reversible redox couples appeared at about 0.31 V for ProDOT-C_4, 0.33 V for ProDOT-C_6 and 0.33 V for ProDOT-C_{10} during repetitive anodic scans (Figure 22).

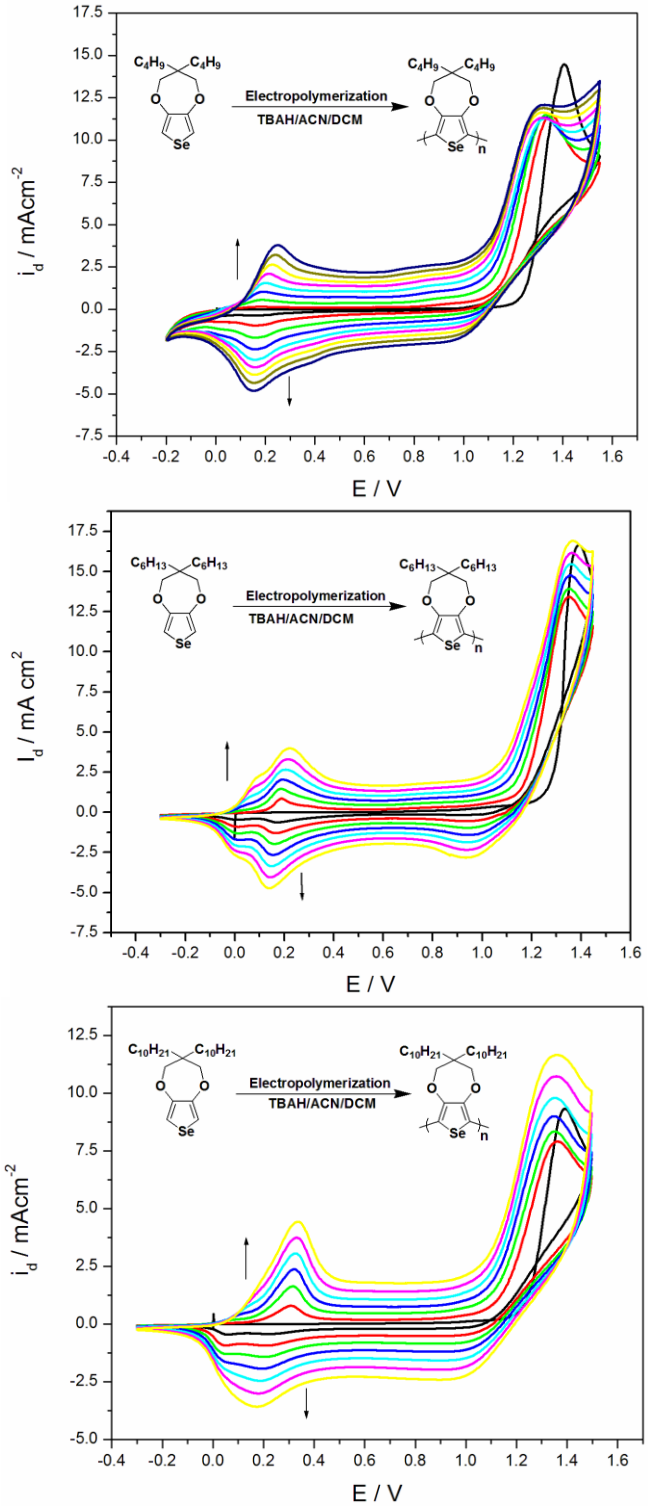

Figure 21. Electropolymerization of 1.0 x 10^{-2} M of ProDOS-C_4, 1.8 x 10^{-2} M of ProDOS-C_6 and 3.5 x 10^{-2} M of ProDOS-C_{10} in 0.1 M TBAH/DCM/ACN (5/95;v/v) at 100 mV/s (vs. Ag/AgCl).

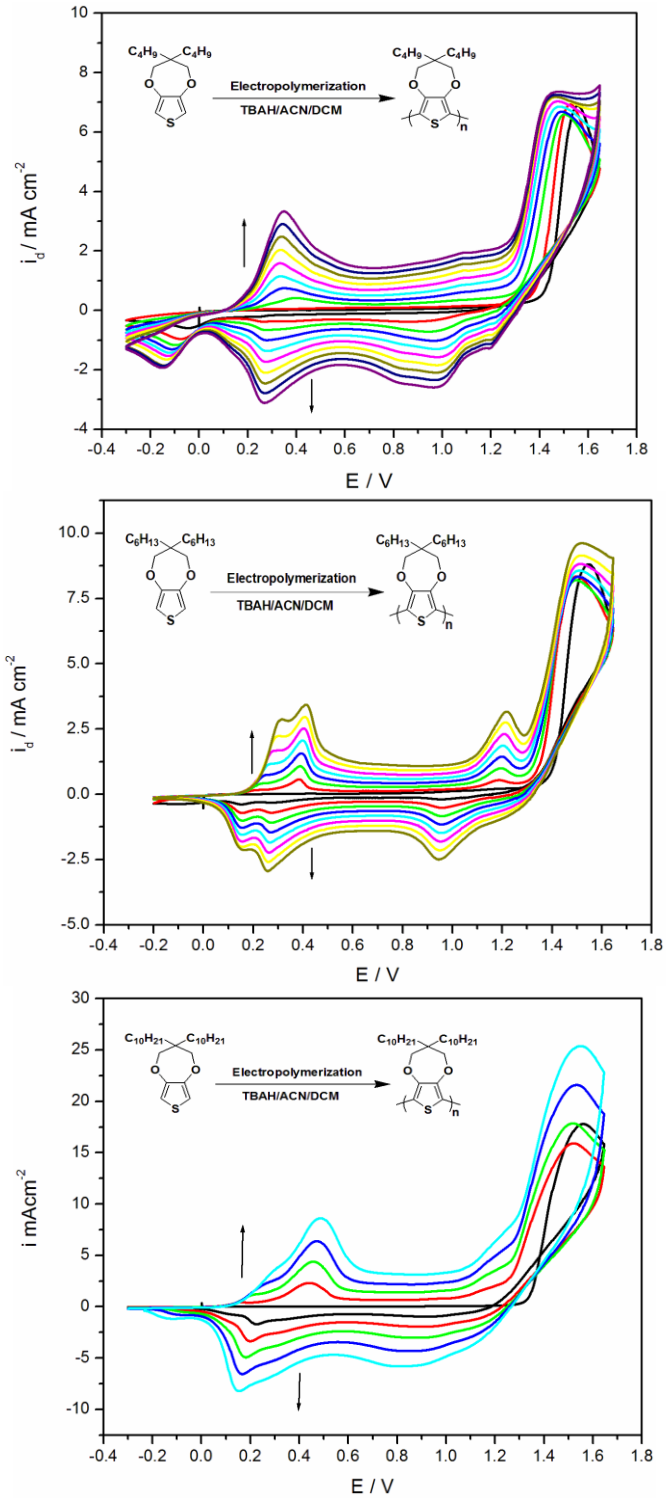

Figure 22. Electropolymerization of 1.5 x 10^{-2} M of ProDOT-C_4, 1.3 x 10^{-2} M of ProDOT-C_6 and 3.3 x 10^{-2} M of ProDOT-C_{10} in 0.1 M TBAH/DCM/ACN (5/95,v/v) at 100 mV/s (vs. Ag/AgCl).

3.2. Electrochemical Properties of Polymers

In endevours to compare behaviors of PProDOS-C_n and PProDOT-C_n polymer films, the obtained polymers via repetitive cycles were scanned anodically in a monomer free electrolytic solution containing 0.1 M TBAH/ACN. PProDOS-C_4, PProDOS-C_6, and PProDOS-C_{10} exhibited single and well-defined reversible redox couples at 0.19 V, 0.17 V and 0.29 V, respectively. These potentials were lower than those of PProDOT-C_4 (0.39 V), PProDOT-C_6 (0.30 V) and PProDOT-C_{10} (0.40 V) under similar conditions (Figure 23), which also confirms the electron-rich nature of PProDOS-C_n when compared to PProDOT-C_n.

Morever, in order to investigate the effect of the alkyl side groups on the redox process of the polymer backbone, electrochemical behaviors of PProDOS-C_n films were compared. It was observed that hexyl substitutents on the polymer backbone decrease the oxidation potential of the polymers (Figure 24). The same behaviors were also observed for PProDOT-C_n (Figure 25).

In order to prove if the reduction potentials that appear around 0.2 V in the CV of PProDOS-C_n films due to the first oxidation potentials or not, waveclipping was performed after the observation of first oxidation potentials (Figure 26). As it can be seen from the experimental results, the reductions around 0.2 V can be attributed to the first oxidation peaks of the polymers. In addition, polymer films showed capacitance properties, no appreciable change in current intensity as a function of potential, approximately between 0.4 V and 1.0 V (Figure 26).

To determine whether redox process is diffusional or not, variation of peak currents as a function of voltage scan rates were also investigated. It was observed that current responses of PProDOS-C_n and PProDOT-C_n were directly proportional to scan rate as illustrated in Figure 27 and 28. As a result, this linearity confirmed that the processes were non-diffusional redox processes. Moreover, the linear increases also demonstrated a well-adhered electroactive polymer films on the electrode surface.

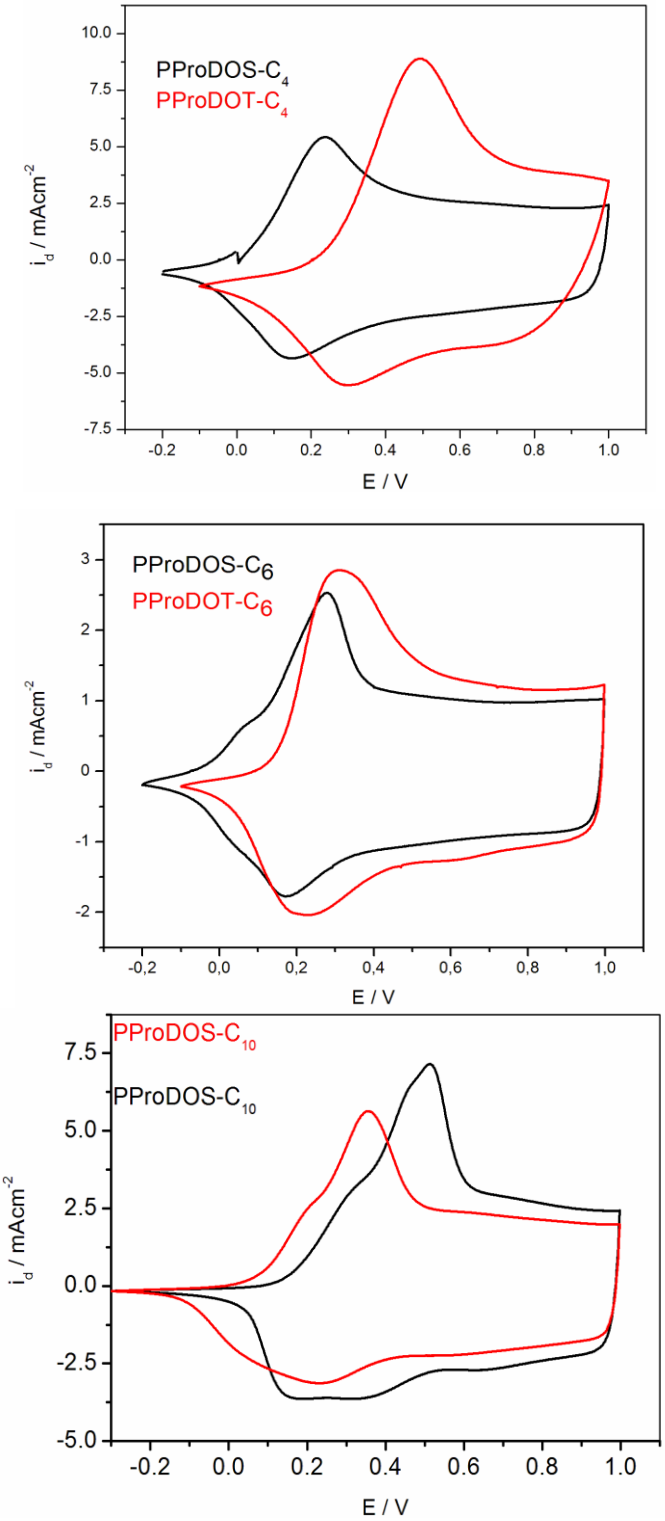

Figure 23. Comparison of cyclic voltammograms of PProDOS-C_n (n = 4, 6, 10) and PProDOT-C_n (n = 4, 6, 10) films on a Pt disk electrode in 0.1 M TBAH/ACN at 100 mV/s (vs. Ag/AgCl).

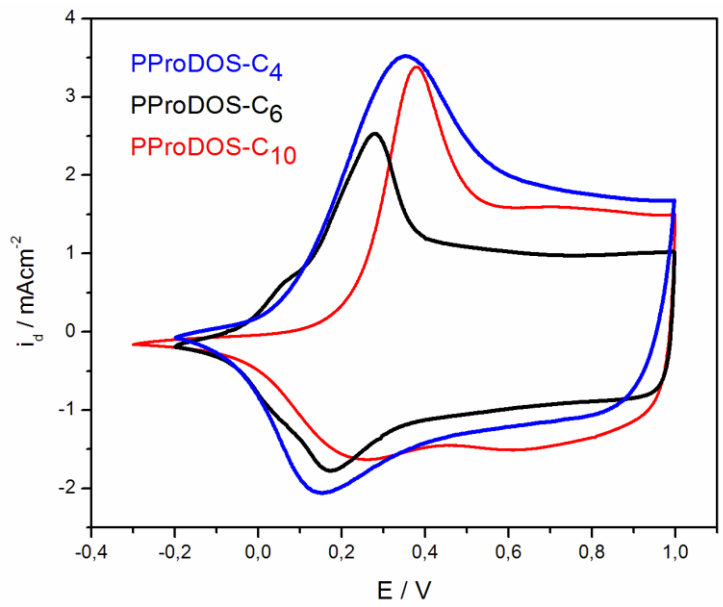

Figure 24. Cyclic coltammograms of PProDOS-C_n (n= 4, 6, 10) films on a Pt disk electrode in 0.1 M TBAH/ACN at 100 mV/s (vs. Ag/AgCl).

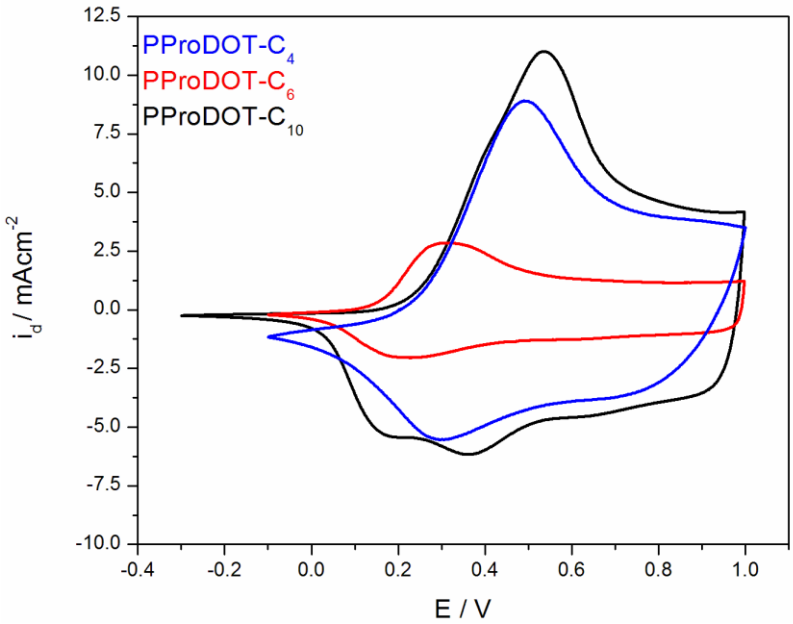

Figure 25. Cyclic voltammograms of PProDOT-C_n (n= 4, 6, 10) films on a Pt disk electrode in 0.1 M TBAH/ACN at 100 mV/s (vs. Ag/AgCl).

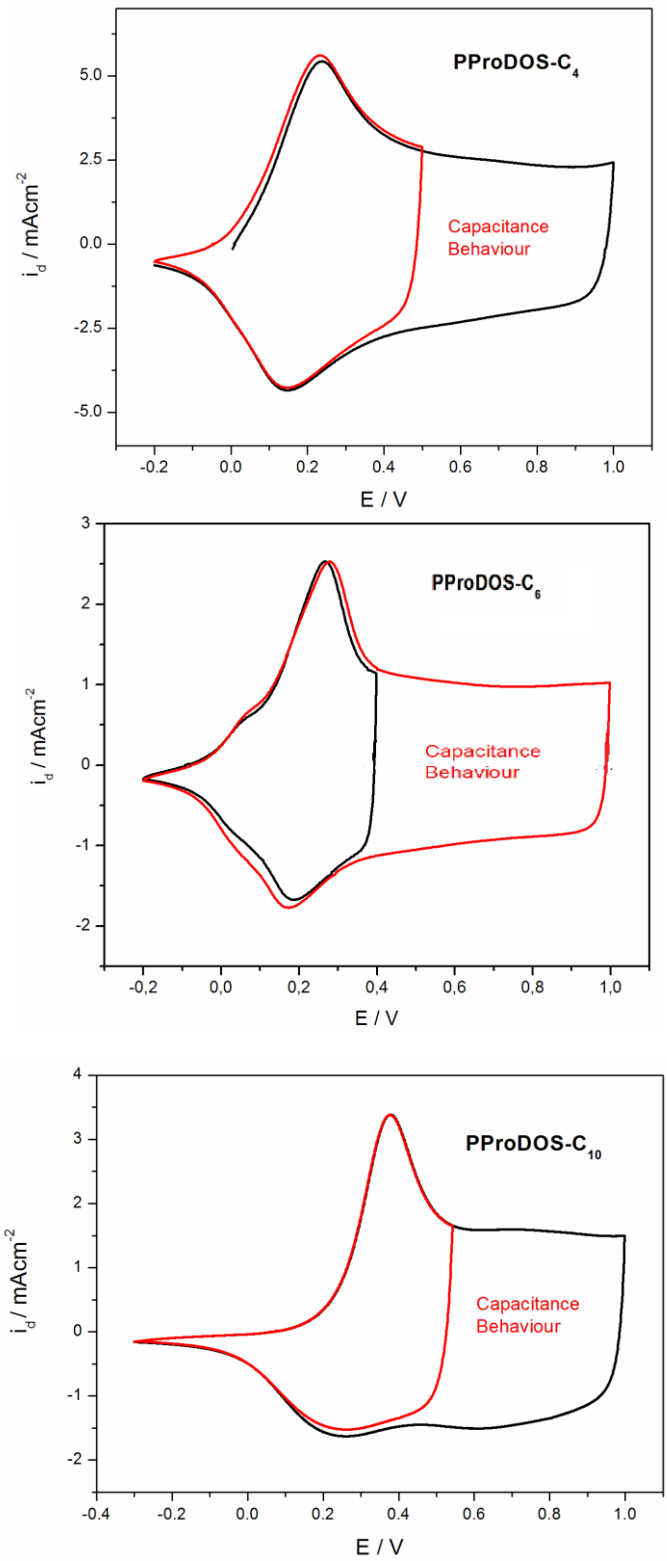

Figure 26. Cyclic voltammograms and capacitance properties of PProDOS-C_n films on a Pt disk electrode in 0.1 M TBAH/ACN at 100 mV/s (vs. Ag/AgCl)

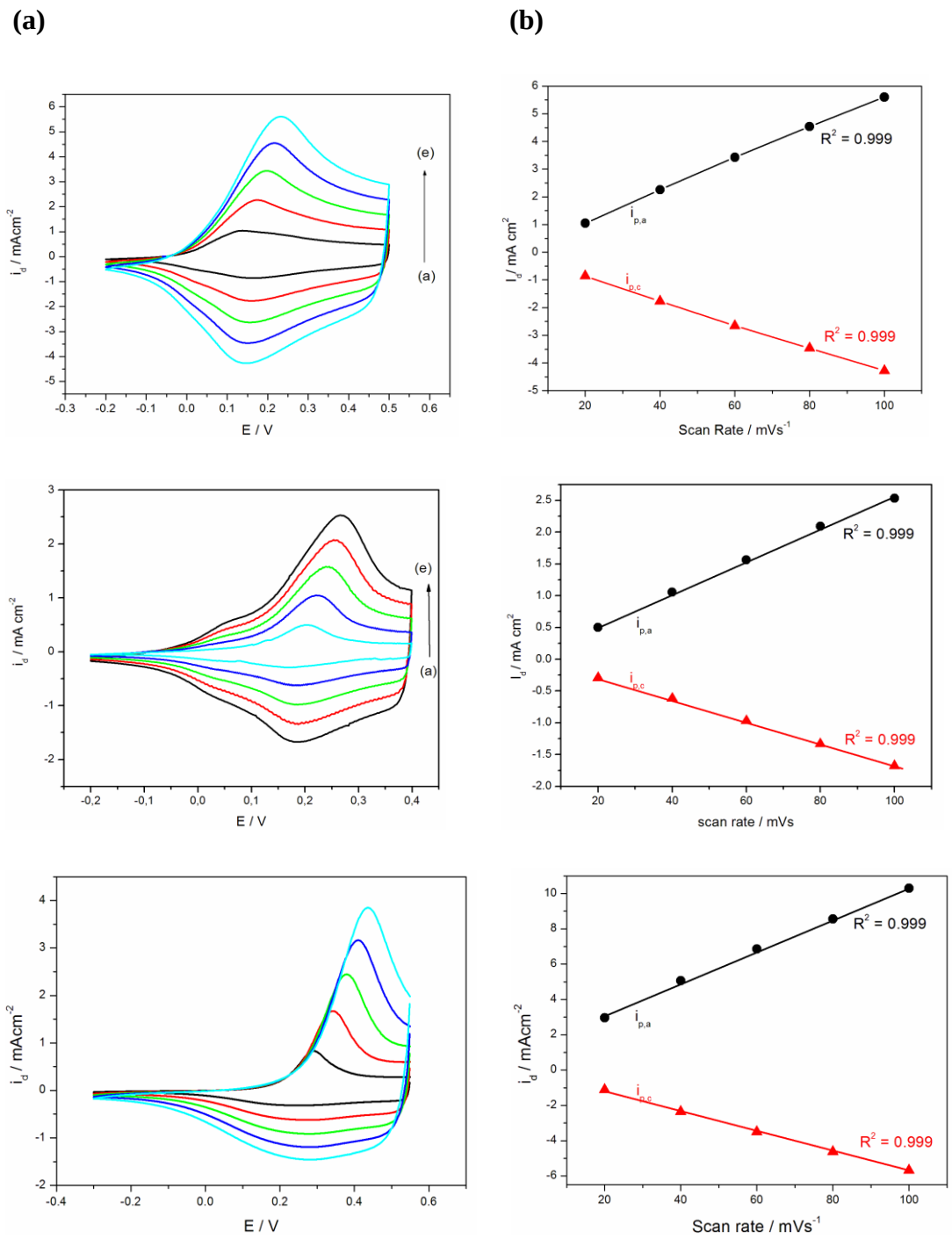

Figure 27. (a) Scan rate dependence of PProDOS-C_n (n = 4, 6, 10) film on a Pt disk electrode in 0.1 M TBAH/ACN at (a) 20 mV/s, (b) 40 mV/s, (c) 60mV/s, (d) 80 mV/s and (e) 100 mV/s. **(b)** Relationship of anodic ($i_{p,a}$) and cathodic ($i_{p,c}$) current peaks as a function of scan rate between neutral and oxidized states of PProDOS-C_n film in 0.1 M TBAH/ACN (vs.Ag/AgCl).

(a) **(b)**

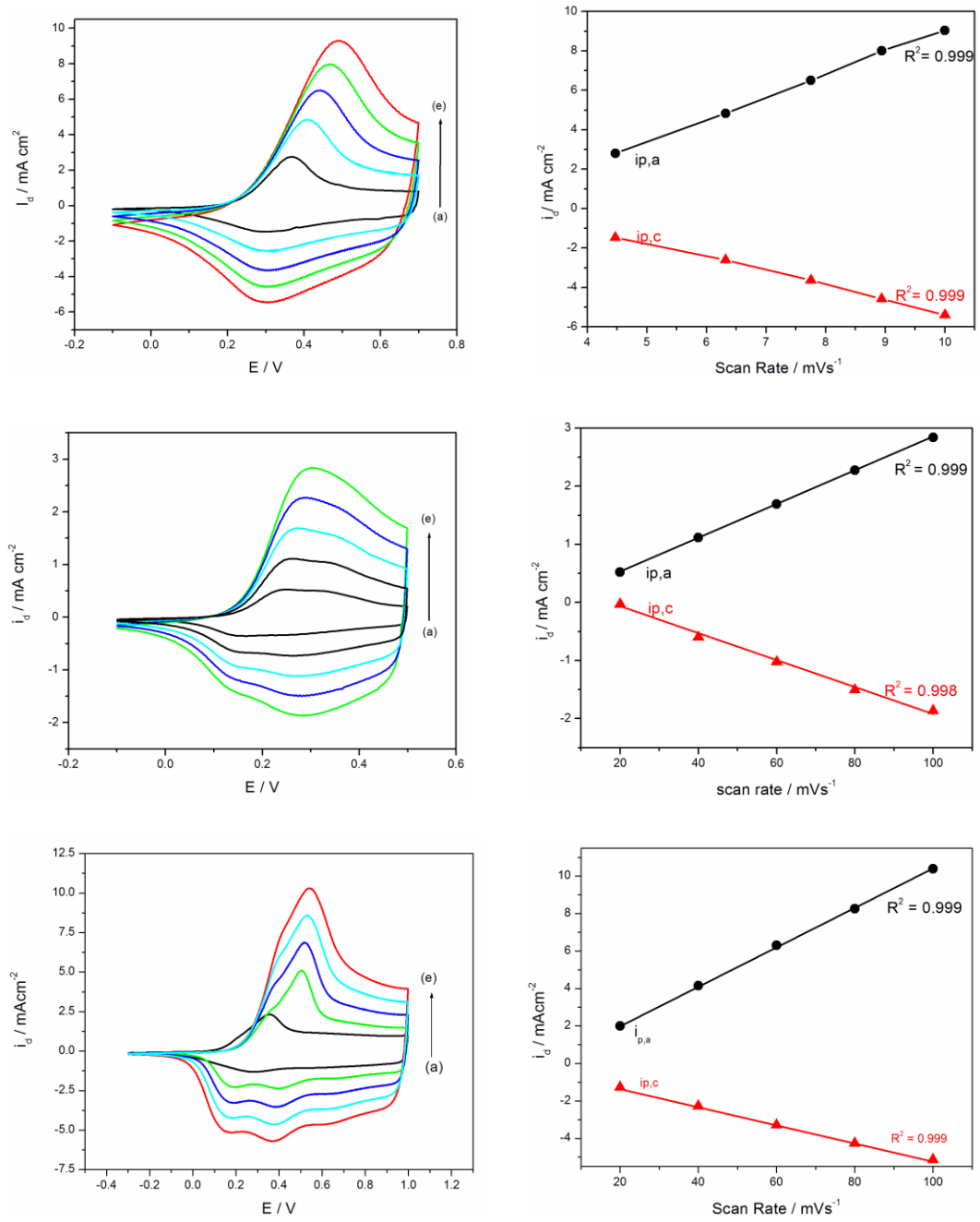

Figure 28. **(a)** Scan rate dependence of PProDOT-C_n (n = 4, 6, 10) film on a Pt disk electrode in 0.1 M TBAH/ACN at (a) 20 mV/s, (b) 40 mV/s, (c) 60mV/s, (d) 80 mV/s and (e) 100 mV/s. **(b)** Relationship of anodic ($i_{p,a}$) and cathodic ($i_{p,c}$) current peaks as a function of scan rate between neutral and oxidized states of PProDOT-C_n film in 0.1 M TBAH/ACN (vs.Ag/AgCl).

3.3. Stability of Polymer Films

For advanced technological applications, the electrochemical stability of the material upon switching or cycling is one of the key parameters. Hence, the stability of PProDOS-C_n (n = 4, 6, 10) films electrodeposited on a Pt disc electrode were investigated by potential scanning between neutral and oxidized states. PProDOS-C_n (n = 4, 6, 10) films were switched using square wave potential between -0.3 V and 0.5 V with an interval time of 2 s and after each 1000 cycles, cyclic voltammograms of polymer films were recorded by CV. As depicted in Figure 29, the polymer films were quite stable and highly robust since they retained 82 % for PProDOS-C_4, 93 % for PProDOS-C_6, 97 % for PPoDOS-C_{10} their electroactivity even after five thousand cycles. It was found that PProDOS-C_n films are more stable than PEDOS and PProDOT-C_n (n = 4, 6, 10) films (retaining about 83 % for PEDOS [65], 82 % for PProDOT-C_4, 91 % for PProDOT-C_6, 68 % for PProDOT-C_{10}) (Figure 30) of electroactivity after five thousands of cycles. Some remarkable features are given below;

- The stability test of PProDOS-C_n (n = 4, 6, 10) films upon cycling were carried out in air, which is generally avoided owing to the fact that the presence of air causes some detrimental effect on the stability of the material

- The PProDOS-C_n (n = 4, 6, 10) films were exceptionally stable in air since almost the same results were obtained with the polymer film even after prolonged standing at ambient conditions (e.g. one-month, and no further trial was done afterwards).

- These results suggest that PProDOS-C_n (n = 4, 6, 10) films may be excellent candidates as electrode materials.

- Also, the long term stability test of PProDOS-C_{10} was done. As depicted in Figure 31, the PProDOS-C_{10} retained 97 % of its electroactivity even after forty thousand cycles. It was exceptionally stable.

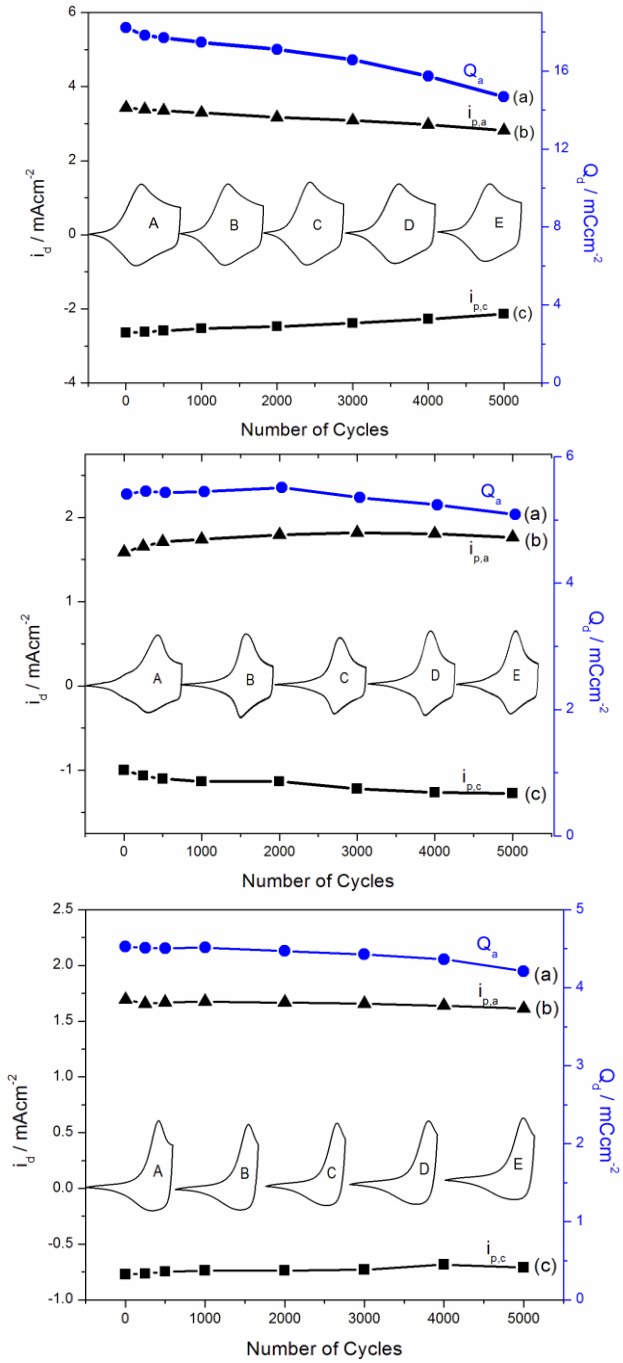

Figure 29. Stability test for PProDOS-C_n (n = 4, 6, 10) films in 0.1 M TBAH/ACN as a scan rate of 60 mVs^{-1} under ambient conditions by CV as a function of : A: 1st; B: 2,000th; C: 3,000th; D: 4,000th; E: 5,000th cycles and by square wave potential between -0.3 V and 0.5 V with an interval time of 2 s; (a) Q_a (anodic charge stored), (b) i_{pa} (anodic peak current), (c) i_{pc} (cathodic peak current).

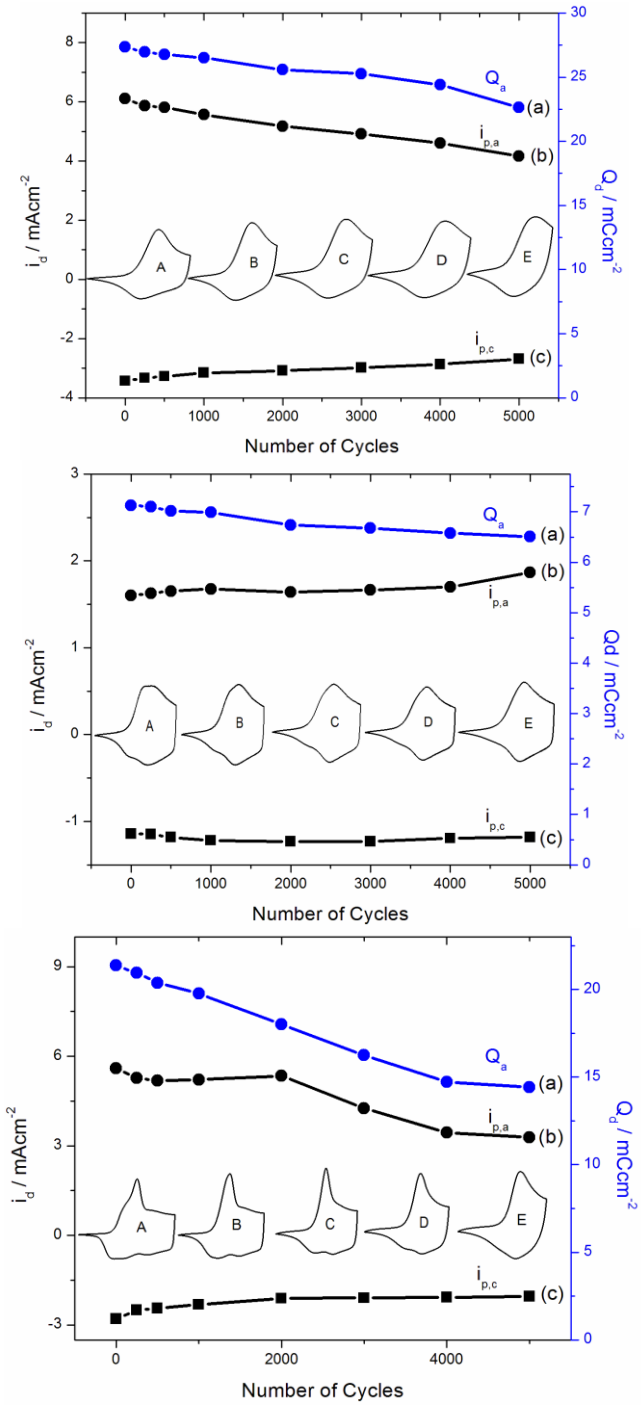

Figure 30. Stability test for PProDOT-C_n (n = 4, 6, 10) films in 0.1 M TBAH/ACN as a scan rate of 60 mVs^{-1} under ambient conditions by CV as a function of : A: 1st; B: 2,000th; C: 3,000th; D: 4,000th; E: 5,000th cycles and by square wave potential between -0.3 V and 0.5 V with an interval time of 2 s; (a) Q_a (anodic charge stored), (b) i_{pa} (anodic peak current), (c) i_{pc} (cathodic peak current).

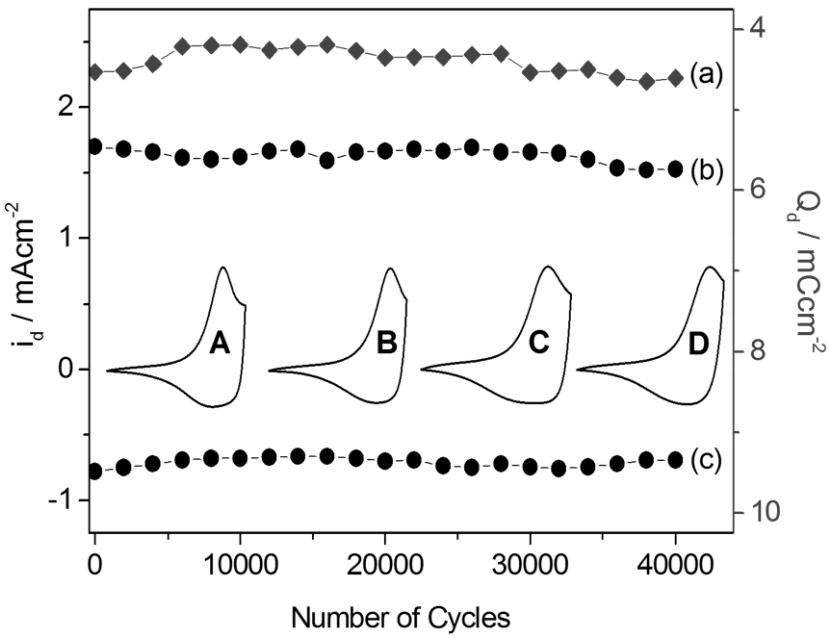

Figure 31. Stability test for PProDOS-C_{10} films in 0.1 M TBAH/ACN as scan rate of 60 mVs^{-1} under ambient conditions by CV as a function of : A: 1st; B: 20,000th; C: 30,000th; D: 40,000th cycles and by square wave potential between -0.3 V and 0.5 V with an interval time of 2 s; (a) Q_a (anodic charge stored), (b) $i_{p,a}$ (anodic peak current), (c) $i_{p,c}$ (cathodic peak current).

3.4. Spectroelectrochemical Properties of Polymers

In the optical spectra of PProDOS-C_4 film there are two absorption bands at 658 nm (1.88 eV), 714 nm (1.74 eV) in its neutral state (Figure 32). Also, PProDOS-C_6 and PProDOS-C_{10} exhibit similar behaviors when compared to PProDOS-C_4 and their data are following; 634 nm (1.95 eV), 698 nm (1.78 eV) with a sholder at 586 nm (2.12 eV) for PProDOS-C_6 and 636 nm (1.95 eV), 697 nm (1.78 eV) with a shoulder at 591 nm (2.10 eV) for PProDOS-C_{10}. Also, PProDOT-C_n (n= 4, 6, 10) films demonstrated similar splitting in the absorbance spectra of their neutral states; 582 nm (2.13 eV), 632 nm (1.96 eV) with a sholder at 537 nm(2.31 eV) for PProDOT-C_4, 572 nm (2.17 eV), 630 nm (1.97 eV) with a sholder at 532 nm(2.33 eV) for PProDOT-C_6, 571 nm (2.17 eV), 622 nm (1.99 eV) for PProDOT-C_{10} (Figure 33). When compared to PProDOT-C_n films (Figure 34) red shifts were observed in optical

spectra of PProDOS-C_n (n= 4, 6, 10) films, which may be attributed to longer chain length of the polymer backbone. As shown in figures 32-34, π-π* transitions of PProDOS-C_n and PProDOT-C_n consist of several peaks, which can be attributed to the vibronic coupling concerning to the formation of a highly regular (solid-state order) polymer backbone containing symmetric alkyl chains [66] or varying effective conjugation lengths in the polymer.

Also, the electronic absorption spectrum of PProDOS-C_n in DCM solution showed hypsochromic shifts (33 nm for PProDOS-C_4, 10 nm PProDOS-C_6 and 17 nm PProDOS-C_{10}) when compared to those of the polymer films on ITO glass slide (in solid state) which might be ascribed to π-π stacking in the solid state (Figure 35).

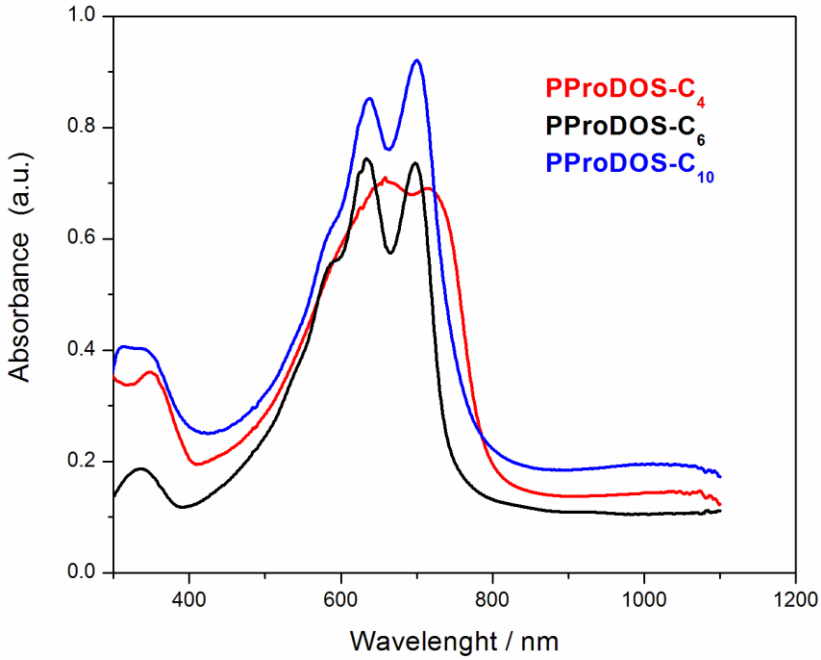

Figure 32. Optical absorption spectra of PProDOS-C_n (n= 4, 6, 10) on ITO in 0.1 M TBAH/ACN at their neutral state.

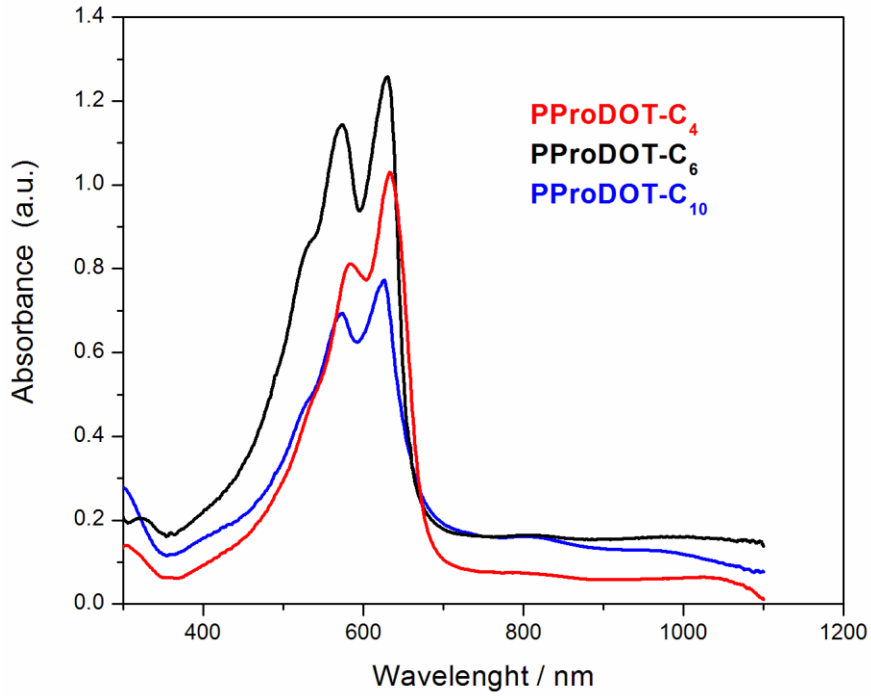

Figure 33. Optical absorption spectra of PProDOT-C_n on ITO in 0.1 M TBAH/ACN at their neutral state.

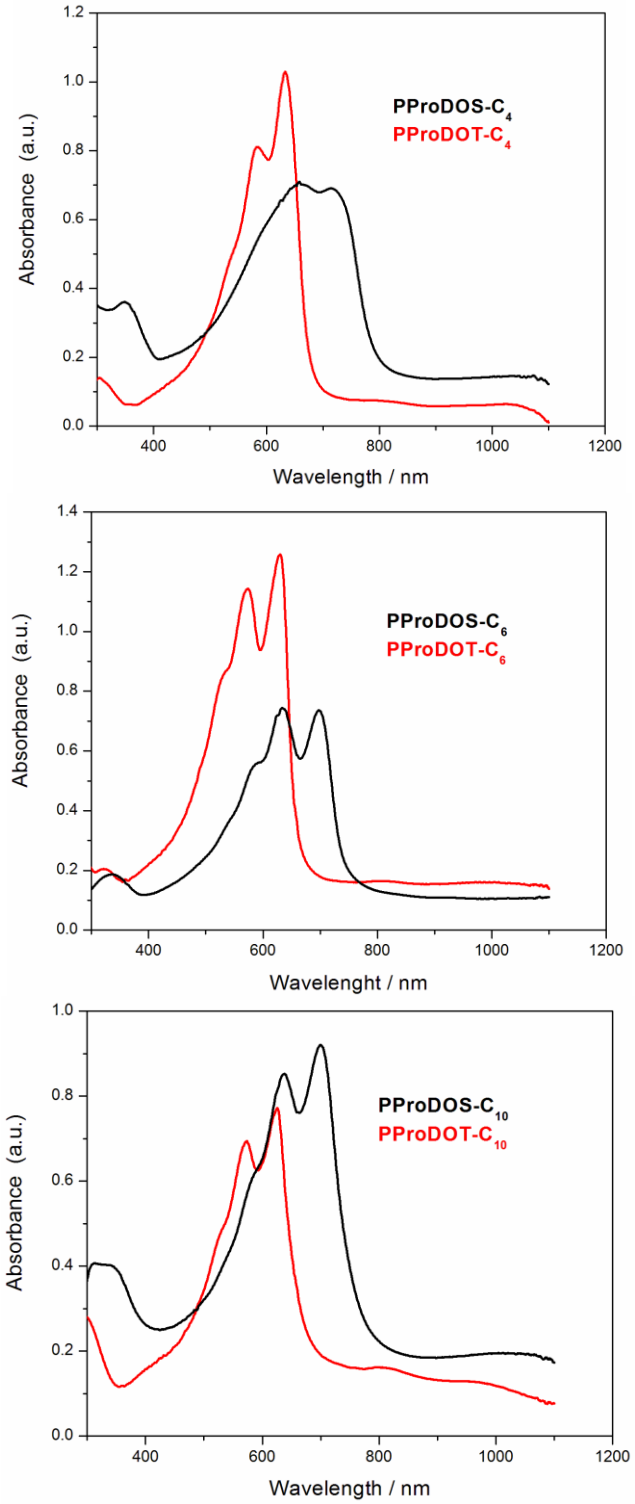

Figure 34. Optical absorption spectra of PProDOS-C_n (n= 4, 6, 10) and PProDOS-C_n (n= 4, 6, 10) on ITO in 0.1 M TBAH/ACN at their neutral state.

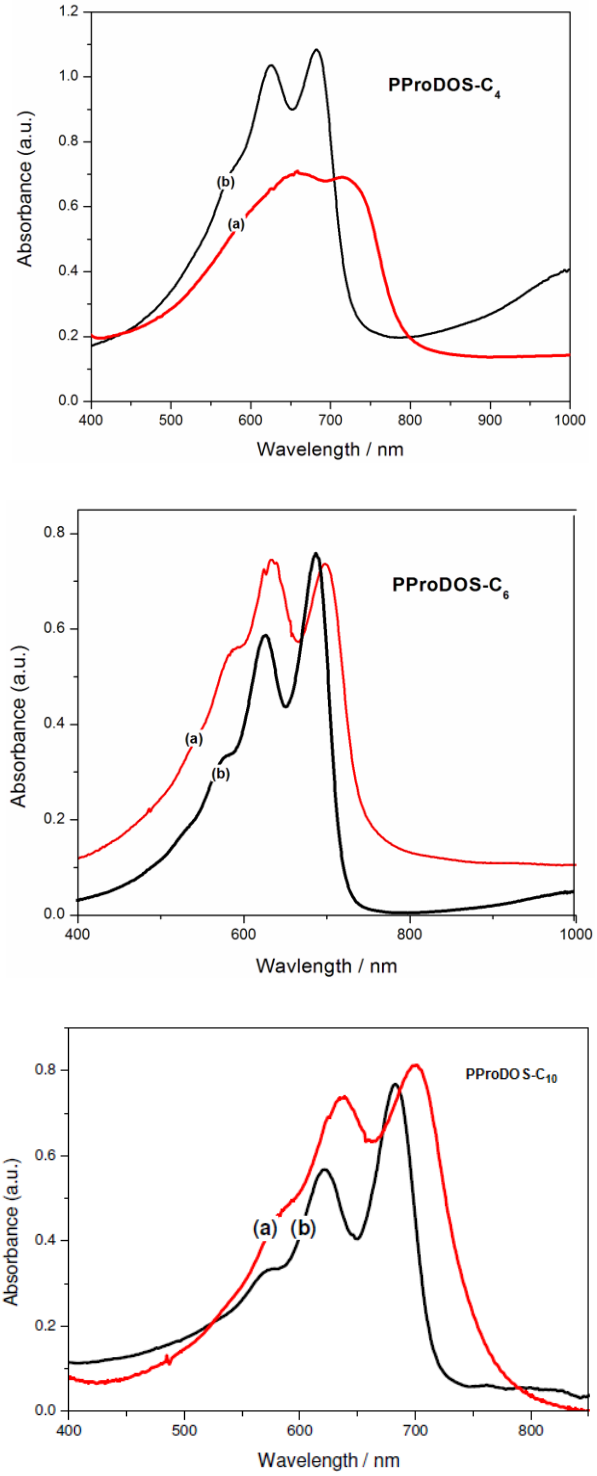

Figure 35. Absorption spectra of PProDOS-C_n film at neutral state (a) coated on ITO electrode and (b) after dissolving in DCM.

The band gap (E_g) values for PProDOS-C_4 on the basis of the low energy end of the π-π* transition at 714 nm was found to be 1.54 eV. Also, the E_g values were found to be 1.63 eV at 696 nm for PProDOS-C_6 and 1.56 eV at 700 nm for PProDOS-C_{10}. These E_g values of PProDOS-C_n are smaller than those of PProDOT-C_n (PProDOT-C_4 (1.83 eV), PProDOT-C_6 (1.88 eV), PProDOT-C_{10} (1.82 eV)), larger than that of PEDOS (1.40 eV) [71] and has nearly the same band gaps of alkyl substituted PEDOS-C_n (1.54 eV) [67].

The optical features of PProDOS-C_n and PProDOT-C_n films were elaborated by recording the changes in the absorption spectra under a variety of voltage pulses after neutralization (Figure 36 and 37). It is important to note that these π-π* transition bands depleted simultaneously upon oxidation with a concomitant increase of new band in the NIR region which was attributed to the formation of charge carriers.

The changes in the optical absorption spectra of PProDOS-C_n film were nicely reflected by a color change from blue to highly transparent state (Tables 1 and 2).

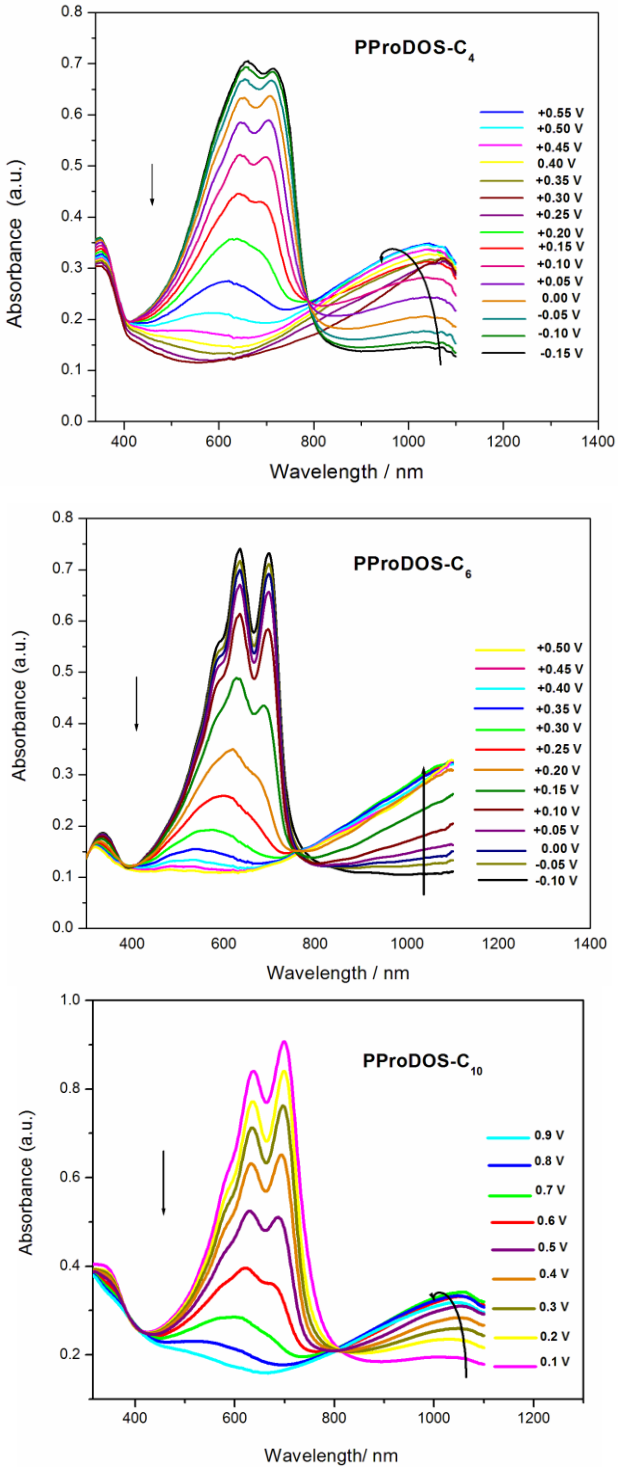

Figure 36. Optical absorption spectra of PProDOS-C_n (n= 4, 6, 10) on ITO in 0.1 M TBAH/ACN at various potentials between -0.15 and 0.55 V for PProDOS-C_4, -0.10 and 0.50 V for PProDOS-C_6, 0.0 and 0.9 V for PProDOS-C_{10}.

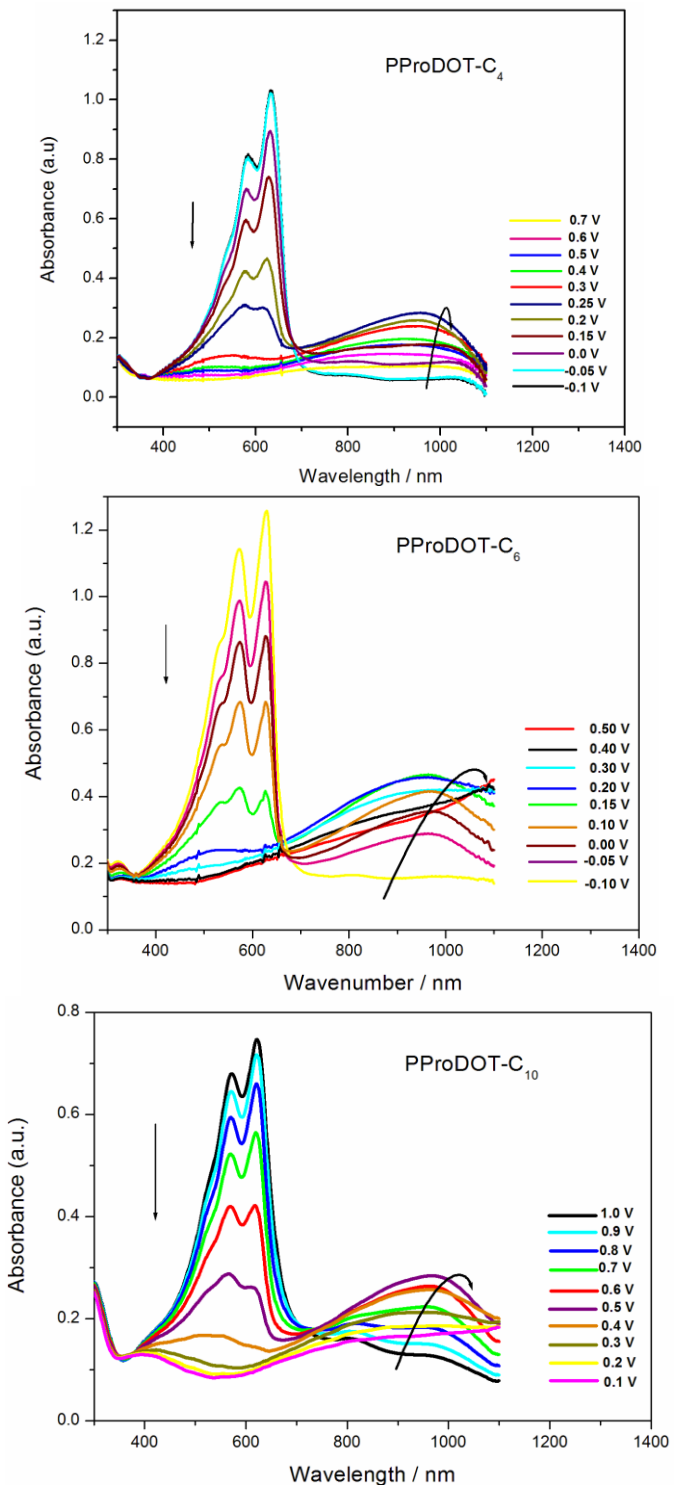

Figure 37. Optical absorption spectra of (a) PProDOT-C_4 (b) PProDOT-C_6 (c) PProDOT-C_{10} on ITO in 0.1 M TBAH/ACN at various potentials between -0.1 and 0.7 V for PProDOT-C_4, -0.10 and 0.50 V for PProDOT-C_6, 0.1 and 1.0 V for PProDOT-C_{10}.

Table 1. L, a, b values and colors of the PproDOS-C_n films at neutral (-0.3 V) and oxidized states(1.0 V).

Polymers	Neutral State				Oxidized State			
	L	a	b	Color	L	a	b	Color
PProDOS-C_4 (a.u= 1.9 at 714 nm)	28.2	8.36	-51.5		76.5	-6.20	-0.45	
PProDOS-C_6 (a.u= 1.5 at 698 nm)	57.3	-13.2	-42.7		91.7	-2.52	-1.30	
PProDOS-C_{10} (a.u= 0.7 at 697nm)	73.7	-11.8	-20.2		91.8	-1.49	3.80	

Table 2. The color change PProDOS-C_n films coated on ITO electrode in 0.1 M TBAH/ACN applied potential chanage between -0.3 V and 0.1 M (vs. Ag wire).

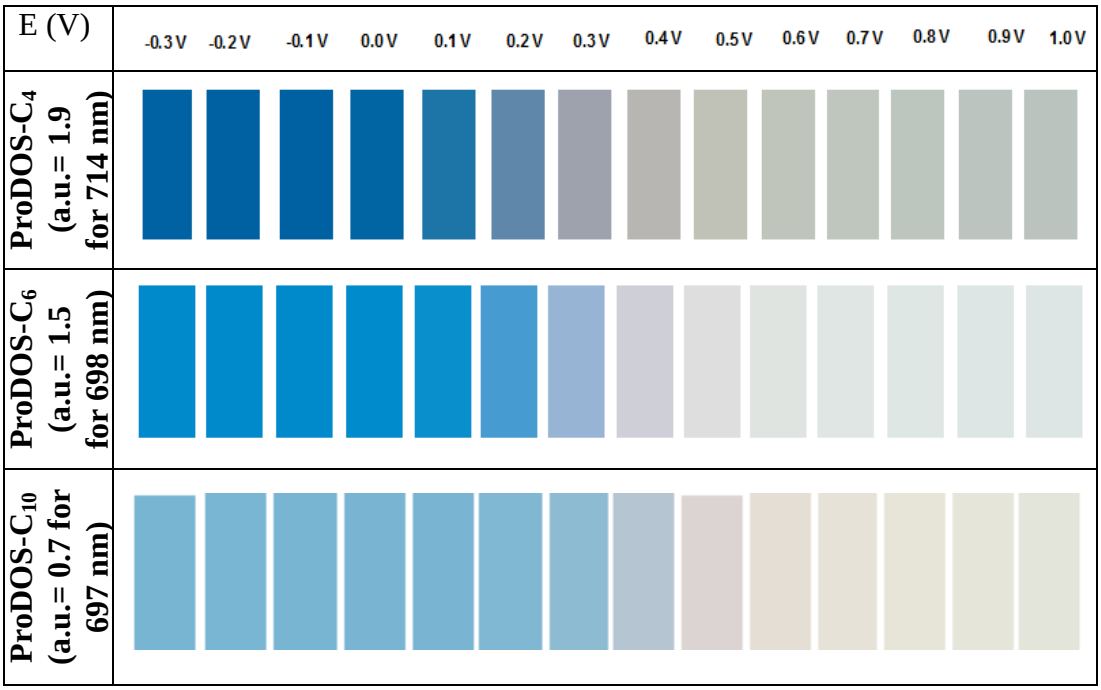

When compared to PEDOT and PProDOT-C_n (Table 3), ProDOS-C_n films exhibit a pure blue color at neutral state due to nearly the absence of absorption between 400 nm and 500 nm. This distinctive property as well as the solubility in organic solvents such as DCM, THF and $CHCl_3$ (Figure 38) makes these polymer films a promising candidate to be amenable for use in electrochromic device applications. It is noteworthy that this color change to transparent state is also a quite significant trait in electrochromic devices and displays along with the blue color of the neutral state since blue color is one leg of the RGB (red, green, blue) color scales.

Table 3. Colors of the PProDOS-C_{10}, PProDOT-C_{10} and PEDOT, on ITO electrodes in their neutral and oxidized state.

	PProDOS-C_{10}	**PProDOT-C_{10}**	**PEDOT**
Neutral State			
Oxidized State			

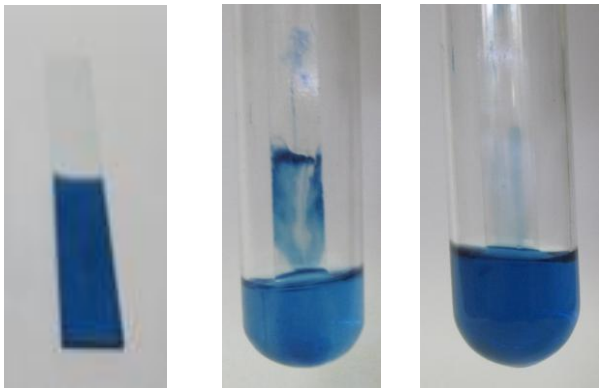

Figure 38. Solubility of PProDOS-C_n film coated on ITO electrode and dissolved in DCM.

The transmissivity can be followed in the change in relative luminance of PProDOS-C_n (Figure 39). These measurments provide a clear quatification of the differences between the colored and neutral states of optoelectronic polymers. The relative luminances of PProDOS-C_n were calculated by the Equation 3-1 where the Y_o is luminance of ITO in monomer free solution. The relative luminances (Δ%T) of PProDOS-C_n were 42 % for PProDOS-C_4, 38 % for PProDOS-C_6 and 18.4 % for PProDOS-C_{10}. All polymers show gradual changes in the relative luminance, which may be attributed to the conformation controlled by the different alkyl chain substituents.

$$\Delta\%Y = (Y/ Y_0) \times 100 \qquad (3\text{-}1)$$

Altough PProDOS-C_n exhibited low luminance in the reduced state, high luminance was observed in the oxidized state (Table 1). Luminance changes in PProDOS-C_n films between redox states are smaller than PEDOT (56%), PProDOT (62 %) PProDOT-C_4 (50%) and PProDOT-C_6 (57%) [64,85].

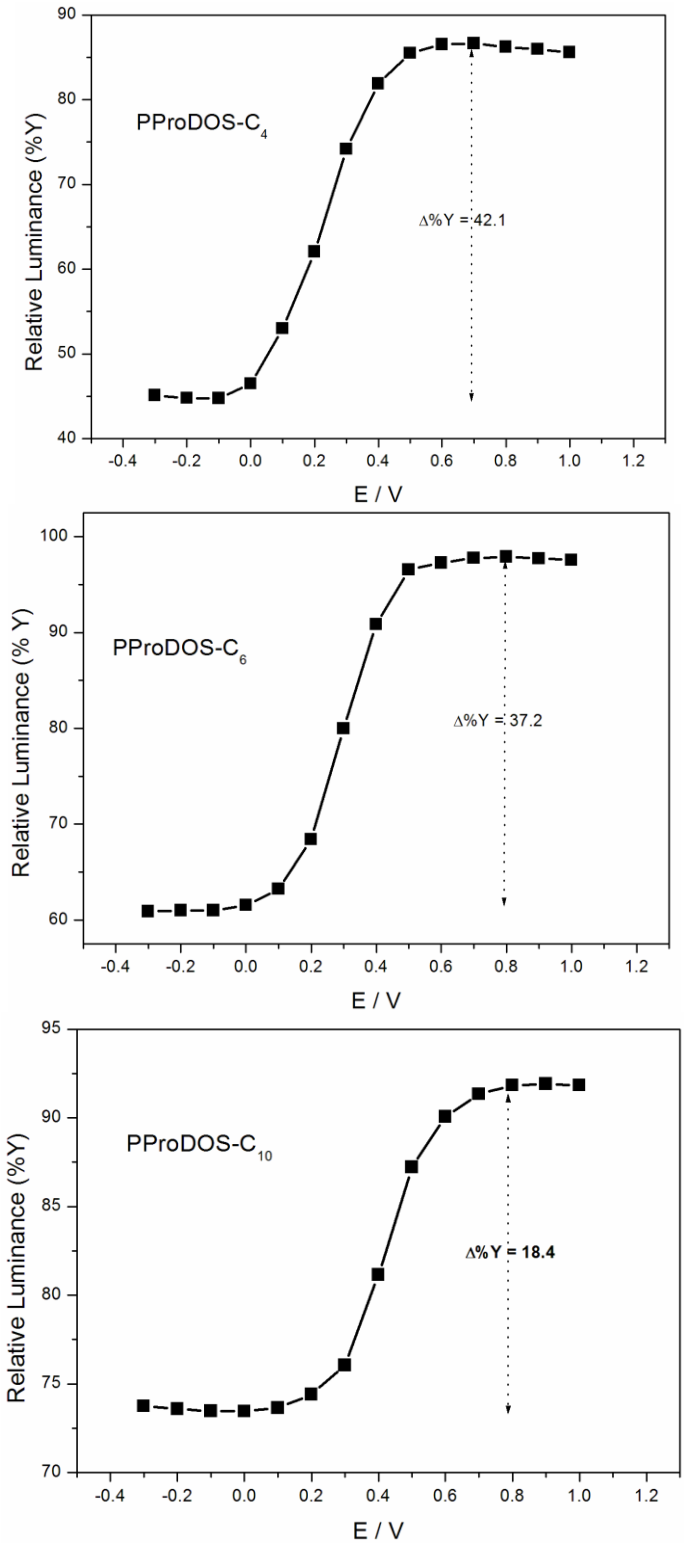

Figure 39. Relative luminance of PProDOS-C_n on ITO in 0.1 M TBAH/ACN under various applied potentials (vs. Ag wire).

3.5. Kinetic Properties of Polymers

The percentage transmittance changes (Δ%T) between the neutral (at 0.0 V) and oxidized states (at 0.55 V) of PProDOS-C_4 film were found to be 55.4 % for 658 nm and 51.3 for 714 nm. Also, Δ%T of PProDOS-C_6 were 59.6 % for 634 nm and 55.5 % for 698 nm between 0.0 V and 0.5 V, Δ%T of PProDOS-C_{10} were 55.5 % for 636 nm and 55.0 % for 697 nm between 0.0 V and 0.9 V (Figure 40). These values are nearly similar to that of PEDOS (55 %) and smaller than those of PEDOS-C_n (67 – 89 %) [64] and PProDOT-C_n (65-73 %). Also, the contrast ratio of PProDOS-C_n kept the stability during the different switching time (Figure 41).

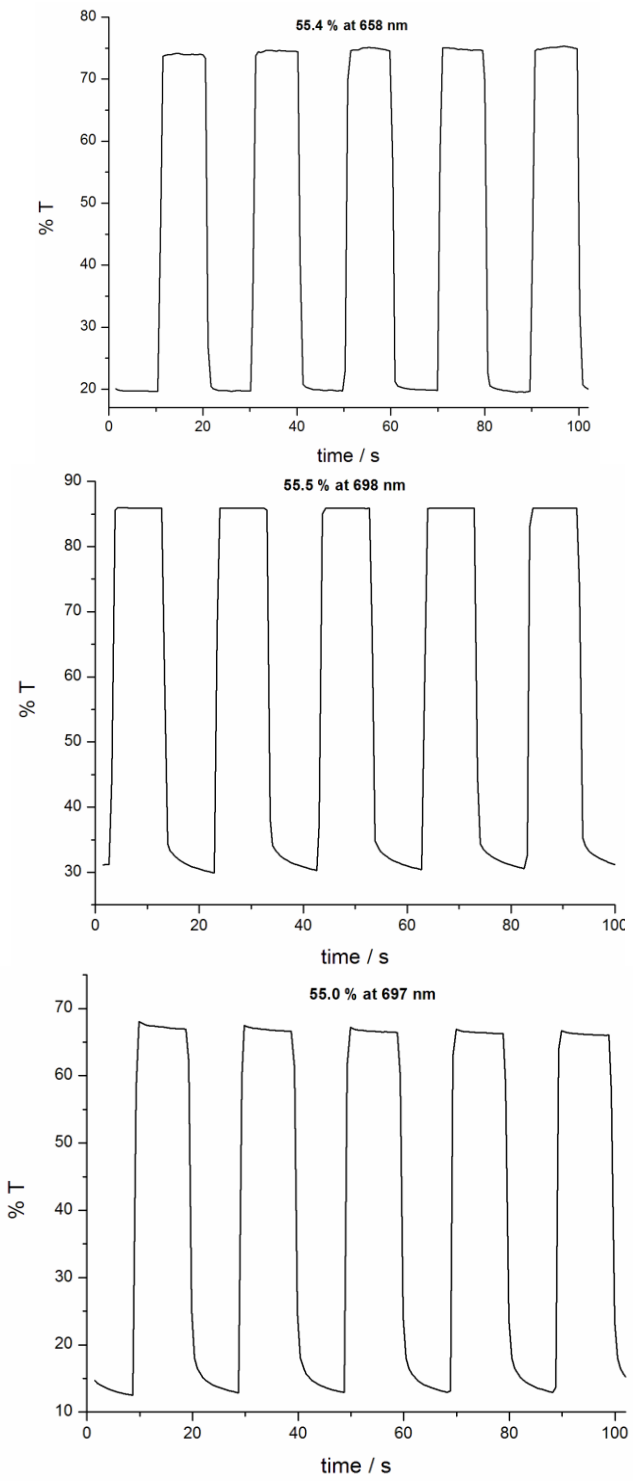

Figure 40. Chronoabsortometry experiments for (a) PProDOS-C_4 film switched between 0.0 V and 0.55 V, (b) PProDOS-C_6 film switched between 0.0 V and 0.50 V, (c) PProDOS-C_{10} film switched between 0.0 V and 0.90 V with an interval time of 10 s on ITO in 0.1 M TBAH/ACN vs. Ag wire.

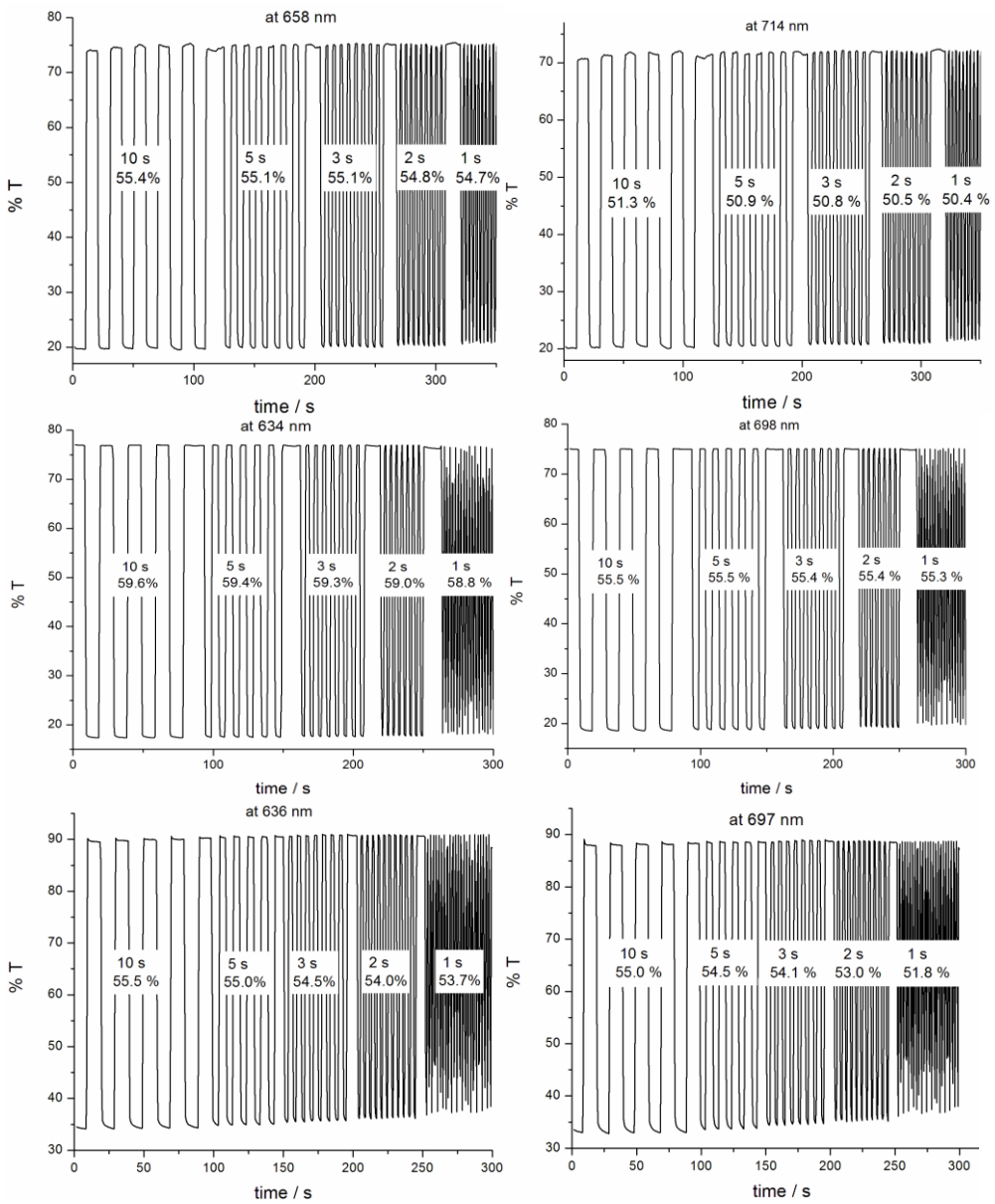

Figure 41. Chronoabsoptometry experiments for PProDOS-C_4, PProDOS-C_6 and PProDOS-C_{10} films on ITO in 0.1 M TBAH/ACN while the polymers were switched in different time (10 s, 5 s, 3 s, 2 s, 1 s) between -0.3 V and 0.55 V for PProDOS-C_4, -0.3 V and 0.50 V for PProDOS-C_6, -0.3 V and 0.5 V for PProDOS-C_{10}.

3.6 Chronoabsorptometry and Chronocoulometry

The CE (at 95 % of the full contrast) was found to be 864 cm^2/C at 658 nm (a response time 1.0 s) for PProDOS-C_4 film (Figure 42), 857 cm^2/C at 634 nm (a response time 1.1 s) for PProDOS-C_6 film and 328 cm^2/C at 636 nm (a response time 1.0 s) PProDOS-C_6 film. The CE (at 95 % of the full contrast) was found to be 850 cm^2/C at 582 nm (a response time 1.2 s) for PProDOT-C_4 film, 514 cm^2/C at 572 nm (a response time 1.0 s) for PProDOT-C_6, and 306 cm^2/C at 622 nm (a response time 0.6) for PProDOT-C_{10}.

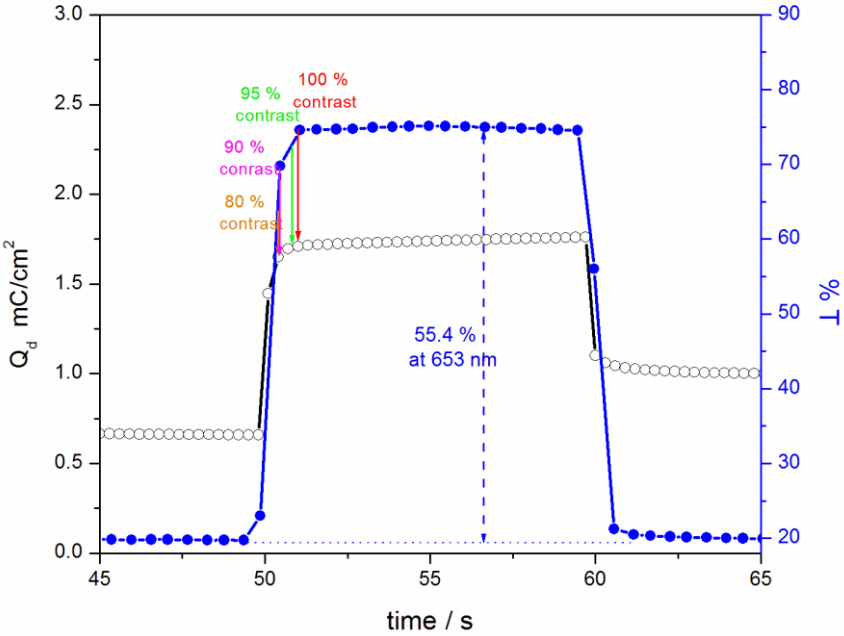

Figure 42. Chronoabsorptometry and chronocoulometry of PProDOS-C_4

Table 4. Optoelectronic properties of PProDOS-C_n films.

	100 % Optical Switch		95 % Optical Switch		90% Optical switch		80 % Optical Switch	
Polymers	Q_d	CE	Q_d	CE	Q_d	CE	Q_d	CE
PProDOS-C_4	0.68	850	0.63	864	0.67	810	0.65	784
PProDOS-C_6	0.53	796	0.52	857	0.52	737	0.51	689
PProDOS-C_{10}	2.67	264	2.22	328	1.92	336	1.73	365

Table 5. Optical and electrochemical properties of ProDOS-C_n and ProDOT-C_n.

	ProDOS-C_4	ProDOS-C_6	ProDOS-C_{10}	ProDOT-C_4	ProDOT-C_6	ProDOT-C_{10}
E_m^{ox} (V)	1.44	1.36	1.39	1.53	1.52	1.55
$E_m^{ox,onset}$ (V)	1.29	1.28	1.24	1.36	1.40	1.38
$E_{p1/2}^{ox}$ (V)	0.19	0.17	0.35	0.39	0.30	0.35
$E_{p1/2}^{ox,onset}$ (V)	0.02	-0.1	0.25	0.24	0.15	0.35
λ_{max} (nm)	658 714	586 shld. 634 698	591 shld. 636 697	537 shld. 582 632	532 shld. 572 630	571 622
E_g (eV)	1.54	1.64	1.58	1.83	1.88	1.82
Δ%T	55.4 (658 nm) 51.3 (714 nm)	59.6(634nm) 55.5 (698nm)	55.5(636 nm) 55.0(697 nm)	68.1(582 nm) 65.1(632 nm)	64.7 (572nm) 64.5 (630nm)	71.5 (571 nm) 73.0 (622 nm)
T_{ox} %	75.5 (658 nm) 71.8 (714 nm)	86.8 (634nm) 86.1 (698nm)	79.6 (636nm) 67.7 (697nm)	74.8 (582nm) 71.1 (632nm)	72.7 (572 nm) 72.8 (630 nm)	88.5 (571 nm) 86.7 (622 nm)
T_{red} %	19.9 (658 nm) 20.5 (714 nm)	33.1 (634nm) 30.6 (698nm)	24.1 (636nm) 12.7 (697nm)	6.68 (582nm) 6.03 (632nm)	7.97 (572 nm) 8.33 (630 nm)	17.0 (571 nm) 13.7 (622 nm)
Color	Blue (neut.) Trasnparent (ox)	Blue (neut.) Trasnparent (ox)	Blue (neut.) Trasnparent (ox)	Violet(neut) Trasnp. (ox)	violet (neut.) Trasnp.(ox)	violet (neut.) Trasnp. (ox)
t_s (s)	1.0	1.1	1.0	1.2	1.0	0.6
ΔOD	0.58 (658 nm) 0.54 (714 nm)	0.42 (634nm) 0.45 (698nm)	0.52 (636nm) 0.73 (697nm)	1.05 (582nm) 1.07 (632nm)	0.96 (572 nm) 0.94 (630 nm)	0.72 (571 nm) 0.80 (622 nm)
$Q_{d95\%}$ (mC/cm^2)	0.63 (714 nm)	0.52 (698 nm)	2.22 (697 nm)	1.26 (632 nm)	1.83 (630 nm)	2.61 (622 nm)
$CE_{95\%}$ (cm^2/C)	864	857	328	850	514	306
HOMO*	-4.45	-4.34	-4.69	-4.68	-4.57	-4.65
LUMO*	-2.91	-2.7	-3.09	-2.85	-2.69	-2.83

* Oxidation potentials are reported vs Fc/Fc+. The energy level of Fc/Fc+ was taken as 4.8 eV below vacuum [83]. The oxidation onset potential of Fc/Fc+ was measured as 0.36 V vs. Ag/AgCl. HOMO energy level was obtained from the onset potential of the oxidation at CV and LUMO energy level was calculated by the substraction of the optical band gap from the HOMO level.

3.7 Molecular Weight Determination

The PProDOS-C_{10} polymer which was obtained by electrochemical polymerization is soluble in THF, so its molecular weight was determined by gas permeation chromotoghrapy (GPC) using a polystyrene as a standart and the measurement yielded 9279 as the average molecular weight. This molecular weight is similar to PProDOT-C_n analoque molecular weight in the literature (Mw= 6000 for PProDOT-C_4, Mw= 6900 for PProDOT-C_6 and Mw= 9300 for PProDOT-C_{10}) [31,86].

CHAPTHER 4

CONCLUSION

A novel series of conjugated monomer (3,3-dialkyl-3,4-dihydro-2H-selenopheno[3,4-b][1,4]dioxephine) was designed and characterized by spectral methods (^{1}H NMR, ^{13}C NMR and FTIR). Furthermore, regioregular and soluble electrochromic polymers, PProDOS-C_n (n= 4, 6 and 10) were synthesized via potential cycling and characterized by voltametric and spectroscopic methods.

The design of new monomers was realized that the replacement of S atom by the Se atom in the identical system did not only provide an access to unique solution processable polymers, but also showed exceptional stability even after prolonged standing at ambient conditions (the PProDOS-C_{10} retained 97 % of its electroactivity even after forty thousand cycles).

In addition they gave low band gap 1.54 eV for PProDOS-C_4; 1.64 eV for PProDOS-C_6; 1.58 eV for PProDOS-C_{10}).

They are the PEC materials which undergo a color change from pure blue (L = 57.3155, a = -13.180, b = -42.6838) to a highly transparent color (L = 91.7403, a = -2.5202, b = -1.3008) with rapid switching times (1s) during oxidation with high coloration efficiency (328 – 864 cm^2/C) and high contrast ratio (55- 59 %). The close analoque of PProDOS-C_n, PProDOT-C_n have same switching time (0.6 – 1.2s) with close coloration efficiency (306 – 850 cm^2/C) and high contrast ratio (65 -73 %).

Like PProDOT-C_n, PProDOS-C_n are soluble in organic solvent, also they are first soluble propylenedioxyselenophene derivatives. As a result, solubility and pure blue color make PProDOS-C_n to be amenable for use in optoelectronic devices. Also, based on the foregoing results, it can be easly concluded that ProDOS-C_n monomers will be one of the most favorable donor units in D-A-D systems instead of their PProDOT analogues.

REFERENCES

1. J. R. Platt, 1961. Electrochromism, a possible change of color producible in dyes by an electric field. J. Chem. Phys. 34:862-863

2. P. M. S Monk., R. J. Mortimer, and D. R. Rosseinsky. 1995. Electrochromism: Fundamentals and applications. Weinheim, Germany: Wiley-VCH.

3. Moritimer, R. J. 1997. Electrochromic materials. Chem. Soc. Rev. 26:147-156.

4. D. R. Rosseinsky, and R. J. Moritimer. 2001. Electrochromic systems and the prospects for devices. Adv. Mater. 13:783-793.

5. P. R. Somani, and S. Radhakrishnan. 2002. Electochromic materials and devices: Present and future. Mater. Chem. Phys. 77: 117-133.

6. S. K. Deb, 1969. Novel electrophotographic system. Appl. Opt. Suppl. 3:192-195.

7. C. K. Chiang, C. R. Fincher, Y. W. Park, A. J. Heeger, H. Shirakawa, E. J. Louis, S. C. Gau, and A. G. MacDiarmid. 1977. Phys. Rev. Lett. 39 (17):1098.

8. H. Shirakawa, E. J. Louis, A. G. MacDiarmid, C. K. Chiang, and A. J. Heeger. 1977. J. Chem. Soc. Chem. Commun. 16:578.

9. (a) H. Shirakawa, 2001. Angew. Chem. Int. Ed. 40 (14):2575; (b) Shirakawa, H. 2002. Synth. Met. 125 (1):3.

10. (a) A. MacDiarmid, 2001. Angwe. Chem. Int. Ed. 40 (14); 2581; (b) MacDiarmid, A. 2002. Synth. Met. 125 (1):11.

11. (a) A. J. Heeger, 2001. Angew. Chem. Int. Ed. 40 (14):2591; (b) Heeger, A. J. 2002. Synth. Met. 125 (1); 23.

12. (a) A. F., Diaz, Kanazawa, K. K., Gardini, G. P. J. Chem. Soc., Chem. Commun. 1979, 635. (b) Diaz, A. F., Castillo, J. I., Logan, J. A., Lee, W. J. Electroanal. Chem. 1981, 129, 115. (c) Lee, K., Heeger, A. J. Synth. Met. 1997, 84, 715.

13. A. Gandini, M. N. Belgancem, Prog. Polym. Sci., 1997, 22 1203.

14. A. F. Diaz, Chem. Scr., 1981, 17, 142.

15. G. Tourillon, F. J. Garnier, J. Electroanal. Chem., 1982, 135, 173.

16. (a) Bayer AG Eur. Patent 339, 334, 1988. (b) F., Jonas, L. Schrader, Synth. Met. 1991, 41-43, 831. (c) G., Heywang, F., Jonas, Adv. Mater. 1992, 4, 116.

17. A. G., MacDiarmid, A., Epstein, J., Farad. Discuss. Chem. Soc. 1989, 88, 317.

18. J. H. Burroughes, D. D. C. Bradley, A. R. Brown, R. N. Marks, K. MacKay, R. H. Friend, P. L. Burn, A. B. Holmes, Nature, 1990, 347, 539.

19. A., Desbene-Monvernay, P.-C., Lacaze, J.-E., Dubois, J. Electroanal. Chem. 1981, 129, 229.

20. P. M. Beaujuge, S. Ellinger, J. R. Reynolds, Nature Materials, 2008, 7, 795.

21. C. M. Amb, P. M. Beaujuge, J. R. Reynolds, Adv. Mater., 2010, 22, 724.

22. P. M. Beaujuge, S. Ellinger, J. R. Reynolds, Adv. Mater., 2008, 20, 2772.

23. G.A. Sotzing, J. R. Reynolds, P. J. Steel, Chem. Mater., 1996, 8, 882.

24. G. A. Sotzing, J. L. Reddinger, A. R. Katriztky, J. Soloducho, R. Musgrave, J. R. Reynolds, Chem. Mater., 1997, 9, 1578.

25. J. A. Irvin, I. Schwendeman, Y. Lee, K. A. Abboud, J. R. Reynolds, J. Polym. Sci. Pol. Chem., 2001, 39, 2164.

26. M. Icli, M. Pamuk, F. Algi, A. M. Onal, A. Cihaner, Chem. Mater, 2010, 22, 4034.

27. T. A. Skotheim, J. R. Reynolds, in Handbook of conducting polymers-conjugated polymers: synthesis, properties and characterization, CRC Press, Boca Raton, FL, 2007.

28. A. Kumar, D. M. Welsh, M. C. Morvant, F. Piroux, K. A. Abboud, J. R. Reynolds, Adv. Mater., 1998, 10, 896.

29. L. B. Groenendaal, J. Friedrich, D. Freitag, H. Pielartzik, J. R. Reynolds, Adv. Mater., 2000, 12, 481.

30. J.-P. Lère-Porte, J. J. E. Moreau, C. Torreilles, Eur. J. Org. Chem., 2001, 1249.

31. D. M. Welsh, L. J. Kloeppner, L. Madrigal, M. R. Pinto, B. C. Thompson, K. S. Schanze, K. A. Abboud, D. Powell, J. R. Reynolds, Macromolecules, 2002, 35, 6517.

32. A. Patra, M. Bendikov, J. Mater. Chem., 2000, 20, 422.

33. A. Patra, Y.H. Wijsboom, G. Leitus, M. Bendikov, Org. Lett., 2009, 11, 1487.

34. (a) S., Asavapiriyonont, G. K., Chandler, G. A., Pletcher, D., Gunawardena, J. Electroanal. Chem. 1984, 177, 229. (b) Inoue, T.; Ymase, T. Bull. Chem. Soc. Jpn. 1983, 56, 985.

35. E. Genius, G. Bidan, A. F. Diaz, J. Electroanal. Chem., 1983, 149, 113.

36. J. Roncali, Chem. Rev., 1992, 92, 711.

37. C. L. Gaupp, PhD thesis, University of Florida, 2002.

38. J. R. Reynolds, S. G. Hsu, H. J. Arnott, J. Polym. Sci Part B Polym. Phys., 1989, 27, 2081

39. G., Zotti, R., Gumbs, Handbook of Organic Conductive Molecules and Polymers, ed. H.S. Nalwa, Editor. 1997, Wiley, Chichester.

40. T. Okada, T. Ogata, M. Ueda, Macromolecules, 1996, 40, 3963.

41. K. Yoshino, R. Hayashi, R. Sugimoto, J. Appl. Phys., 1984, 23, L899.

42. N. Toshima, S. Hara, Prog. Poly. Sci., 1995, 20, 155.

43. (a) Reynolds, J. R.; Ruiz, J. P.; Child, A. D.; Navak, K.; Marynick, D. S. Macromolecules 1991, 24, 678. (b) Reynolds, J. R.; Child, A. D.; Ruiz, J. P.; Hong, S. Y.; Marynick. D.S. Macromolecules 1993, 26, 2095.

44. P. Camurlu, PhD thesis, Middle East Technical University, 2006.

45. A. Malinauskas, Polymer, 2001, 42, 3957.

46. M. Salmon, K. K. Kanazawa, A. F. Diaz, M. Krounbi, J. Polym. Sci, 1982. 20: p. 187.

47. R. H. Baughman, J. L. Bredas, R. R. Chance, R. L. Elsenbaumer, L. W. Shacklette, Chem. Rev., 1982, 82, 209.

48. B. Yigitsoy, M.S. thesis, Middle East Technical University, 2006.

49. J.-L., Bredas, G. B. Street, Acc. Chem. Res. 1985, 18, 1309.

50. P. J. Nigrey, A. G. MacDiarmid, A. J. Heeger, J. Chem. Soc.-Chem. Commun., 1979, 594.

51. D.C., Triverdi, In Handbook of Organic Conductive Molecules and Polymers, Vol. 2, Nalwa, H. S., Ed.; Wiley: Chichester, UK, 1997, pp 505-572.

52. (a) T., Kobayashi, H., Yoneyama, Tamura, H. J. Electroanal. Chem. 1984, 177, 293. (b) Chinn, D.; DuBow, J.; Liess, M. Chem. Mater. 1995, 7, 1504.

53. L. F., Farb & Lack 1998, 10, 93.

54. T., Yamamoto, K., Sanechika, A. J. Yamamoto, Polym. Sci., Polym. Chem. Ed. 1980, 18, 9.

55. S., Yang, P. Olishevski, and M. Kertesz. 2004. Bandgap calculations for conjugated polymers. Synth. Met. 141:171-177.

56. T. C., Chung, J. H. Kaufman, A. J. Heeger, and F. Wudl. 1984. Charge storage in doped poly(thiophene): Optical and electrochemical studies. Phys. Rev. B 30:702-710.

57. G., Tourillon, F., Garnier, J. Phys. Chem. 1983, 87, 2289.

58. G., Dian, G., Barey, B. Decroix, Synth. Met. 1986, 13, 281.

59. (a) G., Tourillon, F., Garnier, J. Electroanal. Chem. 1984, 161, 51. (b) Daosut, G.; Leclerc, M. Macromolecules 1991, 24, 455.

60. M., Dietrich, J., Heinze, G., Heywang, F., Jonas, J. Electroanal. Chem. 1994, 369, 87.

61. E., Aqad, M. V., Lakshmikantham, M. P., Cava, Org. Lett. 2001, 3, 4283.

62. D. Asil, A.M. Önal, A. Cihaner, Chem. Commun., 307-309 (2009).

63. A. Cihaner, F. Algı, Adv. Funct. Mater. 18, 3583 (2008).

64. B. D. Reeves, C. R. G. Grenier, A. A. Argun, A. Cirpan, T. D. McCarley, J. R. Reynolds, Macromolecules, 2004, 37, 7559.

65. D. M., Welsh, A., Kumar, E. W., Meijer, J. R. Reynolds, Adv. Mater. 1999, 11, 1379.

66. K Krishnamoorthy, A. V. Ambade, M. Kanungo, A. Q. Contractor, A. J. Kumar, J. Mater. Chem. 2001, 11, 2909.

67. L. Groenendaal, G. Zotti, P-H. Aubert, S.M. Waybrigth, J. R. Reynolds, Adv. Mater. 2003, 15, 855.

68. H., Kobayashi, H. Cui, Chem. Rev. 2004, 104, 5265-5288.

69. For properties of polyselenophenes, see: (a) Xu, J.; Hou, J.; Zhang, S.; Nie, G.; Pu, S.; Shen, L.; Xiao, Q. J. Electroanal. Chem. 2005, 578, 345– 355. (b) Pu, S.; Hou, J.; Xua, J.; Nie, G.; Zhang, S.; Shen, L.; Xiao, Q. Mater. Lett. 2005, 59, 1061–1065. (c) Tourillon, G.; Dartyge, E.; Guay, D.; Mahatsekake, C.; Andrieu, C. G.; Bernstorff, S.; Braun, W. J. Electrochem. Soc. 1990, 137, 1827–1832.

70. S. S. Zade, N. Zamoshchik and M. Bendikov, Chem. –Eur. J., 2009, 15, 8613.

71. A. Patra, Y.H. Wijsboom, S.S. Zade, M. Li, Y. Sheynin , G. Leitus, M. Bendikov, J. Am. Chem. Soc., 2008, 130, 6734.

72. M. Li, A. Patra, , Y. Sheynin, M.Bendikov, Adv. Mater., 2009, 21, 1707.

73. M. Li, Y. Sheynin, A. Patra, M. Bendikov, Chem. Mater., 2009, 21, 2482.

74. A. Argun, P.H.Aubert, B. C. Thompson, I. Schwendeman, C. L. Gaupp, J. Hwang, N. J. Pinto, D. B. Tanner, A. G. MacDiarmid, J. R. Reynolds, Chem. Mater., 2004, 16, 4401.

75. A., Dodabalapur, L., Torsi, H. E. Katz, Science 1995, 268, 270.

76. R. H., Friend, R. W., Gymer, A. B., Holmes, J. H., Burroughes, R. N., Taliani, D., Bradley, D. C., Dos Santos, D. A., Bredas, J.-L., Logdlund, M., Salaneck. W. R. Nature 1999, 397, 121.

77. P. Novak, K. Muller, K. S. V. Santhanam, O. Haas, Chem. Rev., 1997, 97, 207.

78. J. M. Pernaut, J. R. Reynolds, J. Phys. Chem. B., 2000, 104, 4080.

79. Handbook of the conducting polymers, T. A. Skotheim, R. L. Elsenbaumer, J. R. Reynolds, Eds. Marcel Dekker: New York, 1998.

80. A. Cirpan, A. A. Argun, C. R. G. Grenier, B. D. Reeves, J. R. Reynolds, J. Mater. Chem., 2003, 13, 2422.

81. P. M. Beaujuge, J. R. Reynolds, Chem. Rev., 2010, 110, 268.

82. W.S. Shin, S.C. Kim, S.-J. Lee, H.S. Jeon, M.-K. Kim, B.V.K. Naidu, S.-H. Jin, J.-K. Lee, J.W. Lee, Y.-S. Gal, J. Polym. Sci. Part A: Polym. Chem., 2007, 45, 1394-1402.

83. R. D., Rauh, S. F. Cogan, Solid State Ionics 1988, 28-30, 1707.

84. K., Bange, T. Bambke, Adv. Mater. 1990, 2, 10.

85. C. L. Gaupp, D. M. Welsh, R.D. Rauh, J. R. Reynolds, Chem. Mater., (2002), 14, 3964-3970.

86. C.B. Nielsen and T. Bjernholm, Macromolecules (2005) 38, 10379-10387.

APPENDIX A

FTIR SPECTRA OF PProDOS-C_n MONOMERS

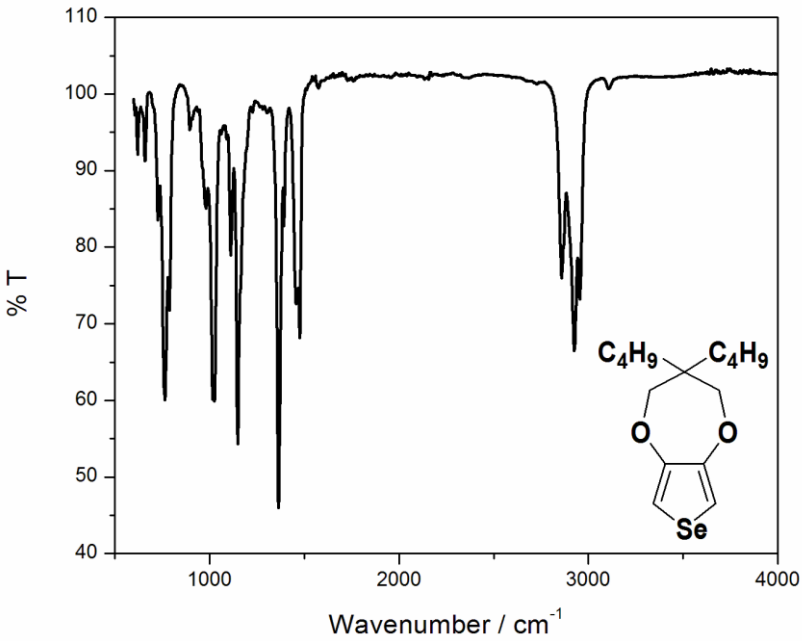

Figure A 1. FTIR spectra of ProDOS-C_4.

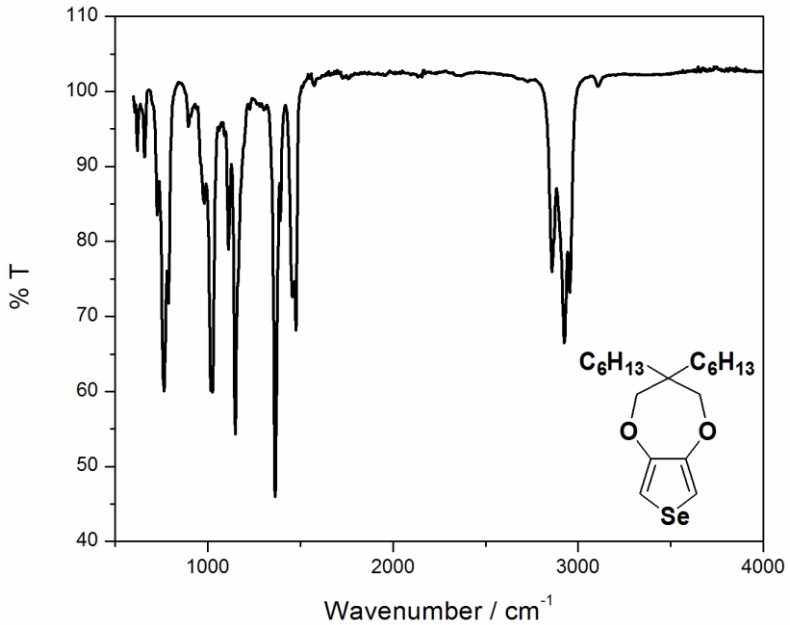

Figure A 2. FTIR spectra of ProDOS-C_6.

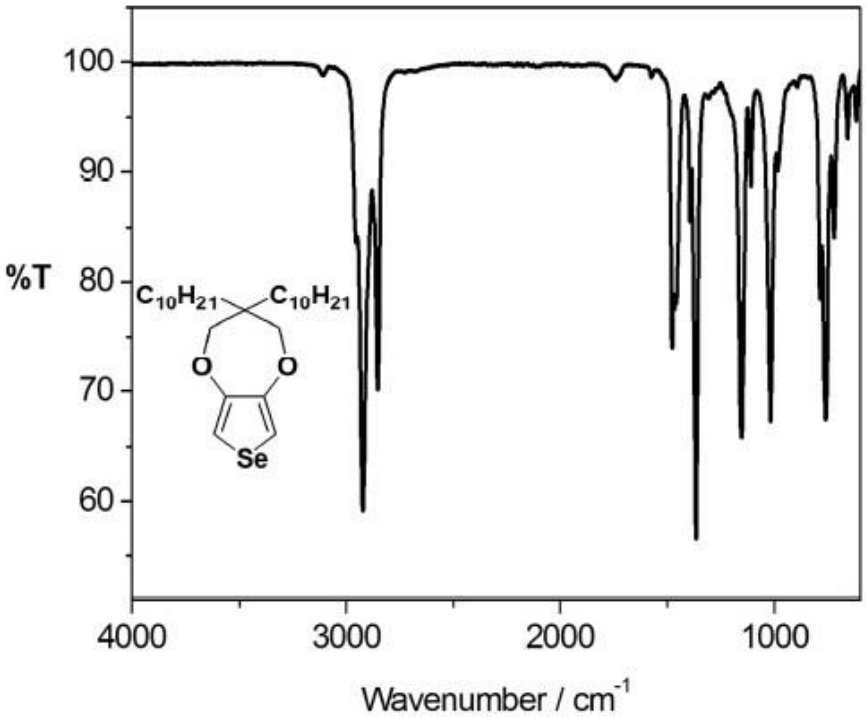

Figure A 3. FTIR of PProDOS-C_{10}.

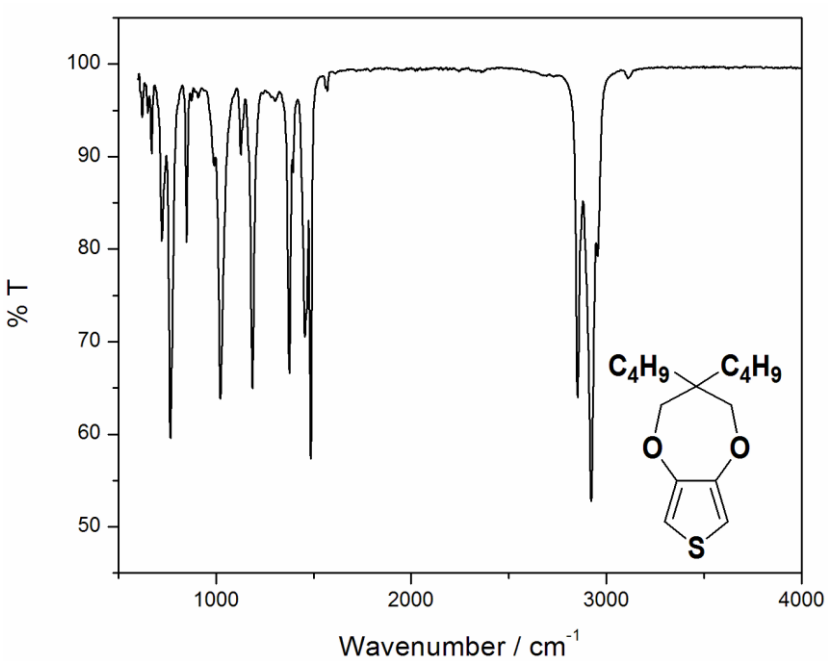

Figure A 4. FTIR of PProDOT-C_4.

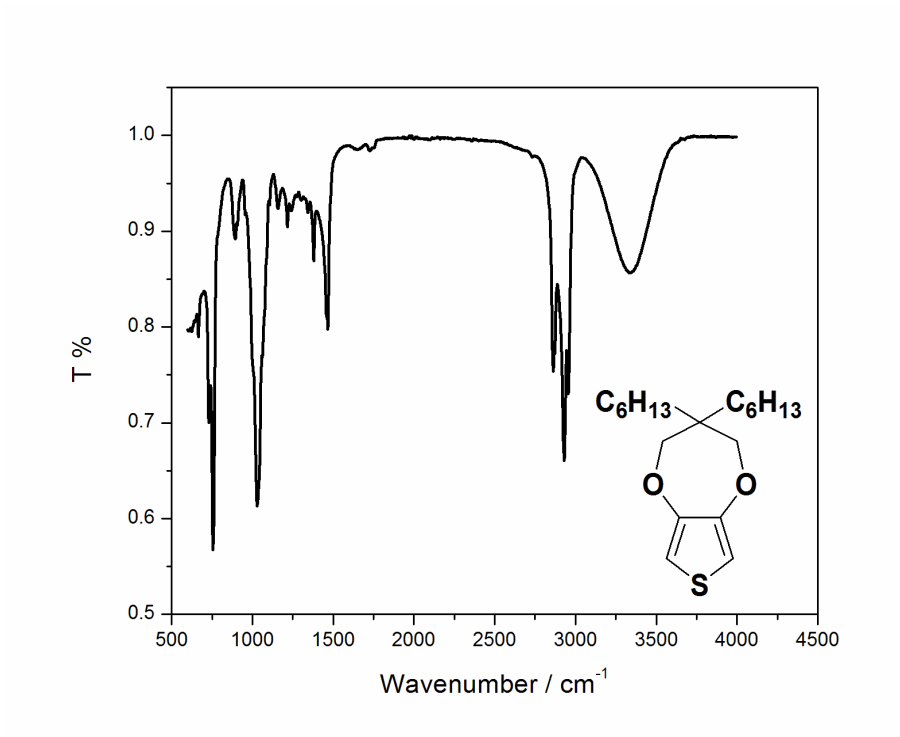

Figure A 5. FTIR of PProDOT-C_6.

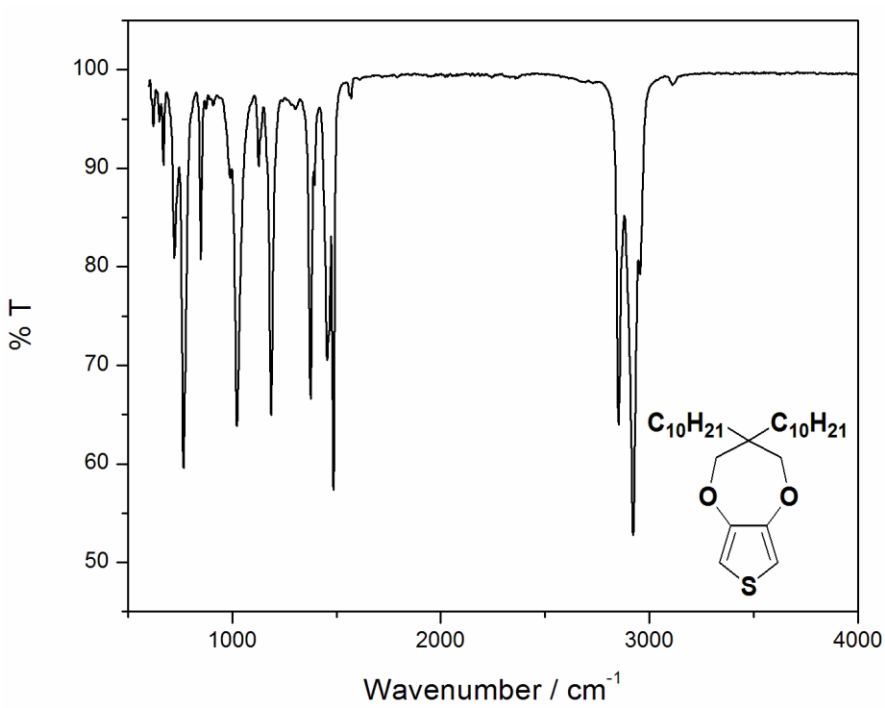

Figure A 6. FTIR of PProDOT-C_{10}.

APPENDIX B

NUCLEAR MAGNETIC RESONANCE SPECTRA OF ProDOS-C_n MONOMERS

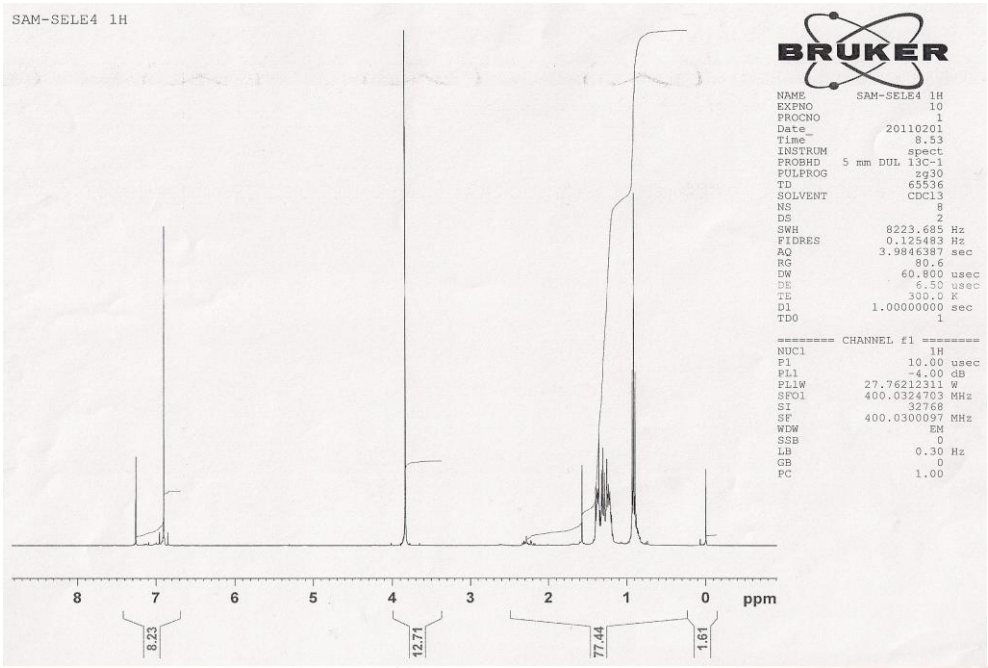

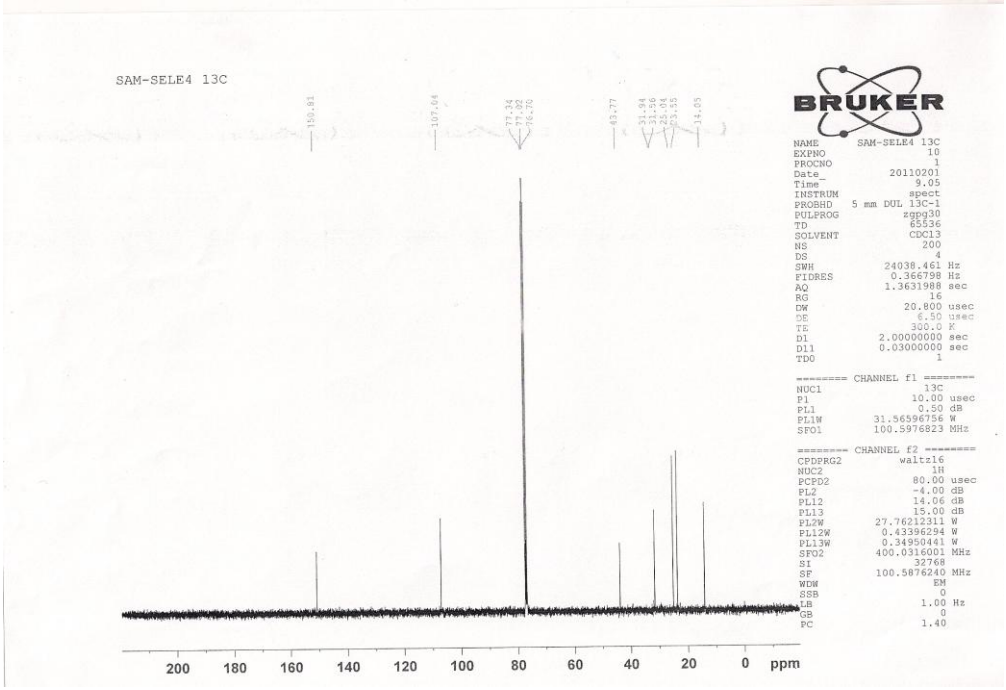

Figure B.1. ^{1}H NMR and ^{13}C NMR of ProDOS-C_4.

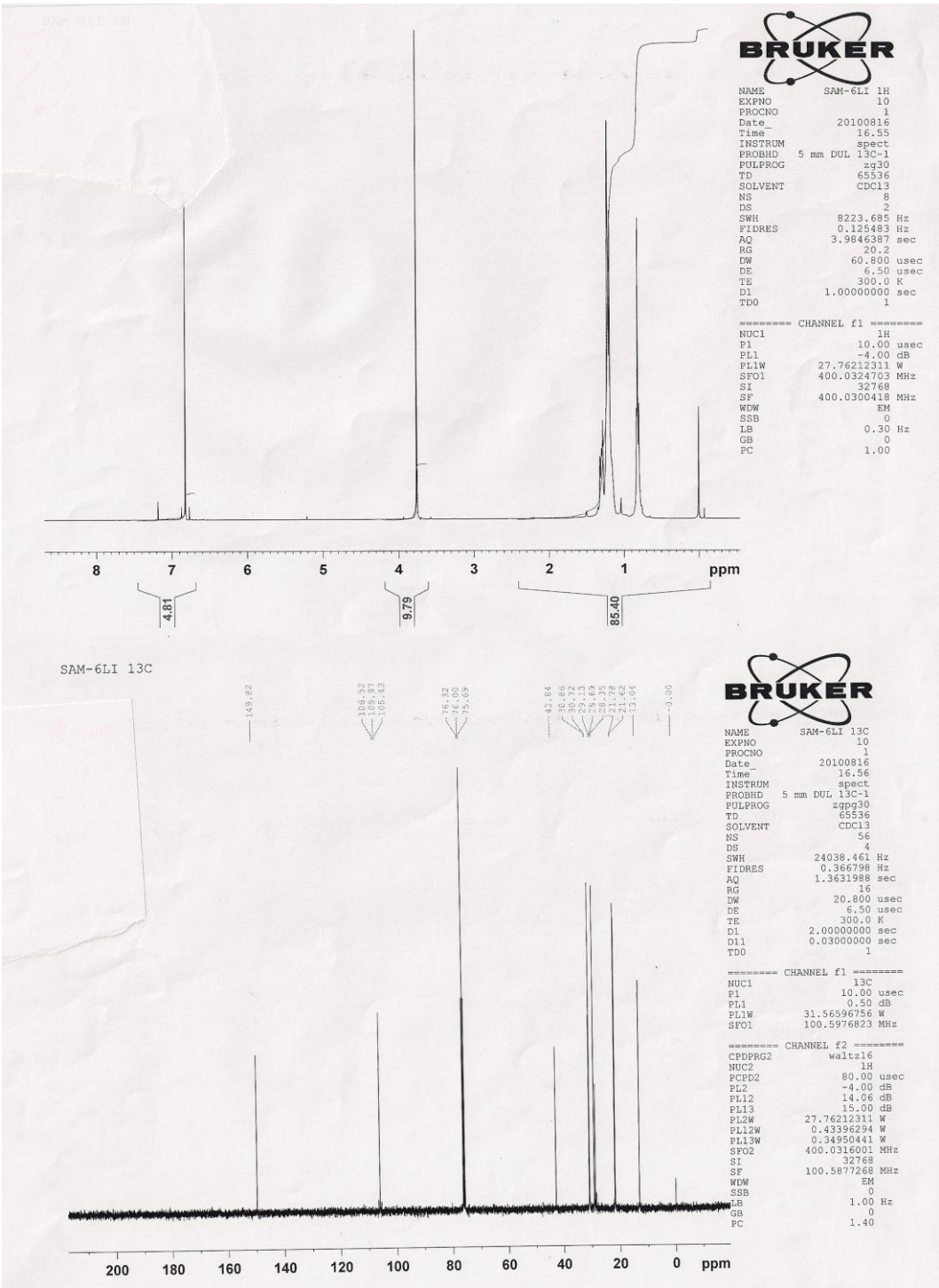

Figure B.2 ^{1}H NMR and ^{13}C NMR of ProDOS-C_6.

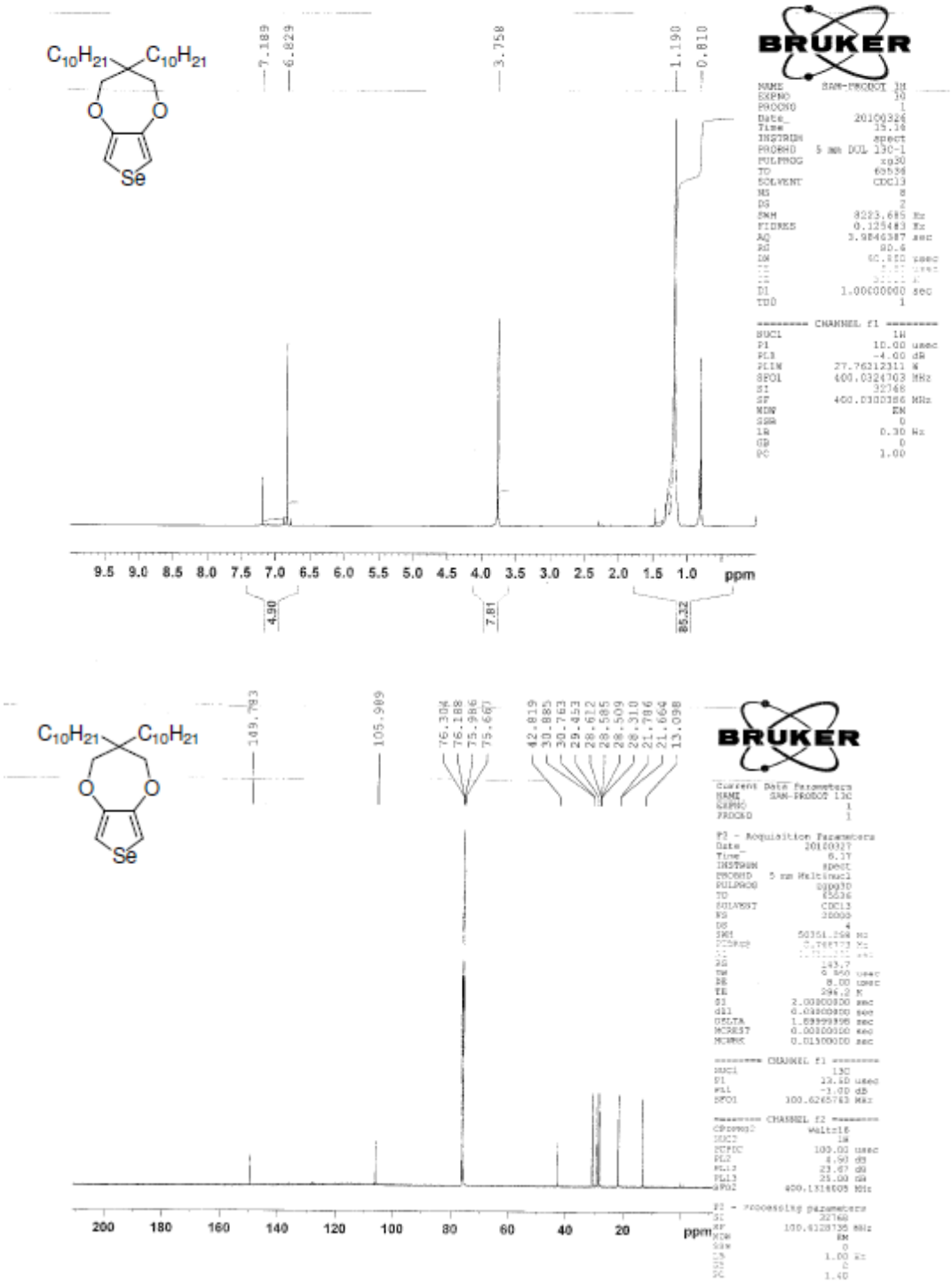

Figure B.3. ^{1}H NMR and ^{13}C NMR of ProDOS-C_{10}.

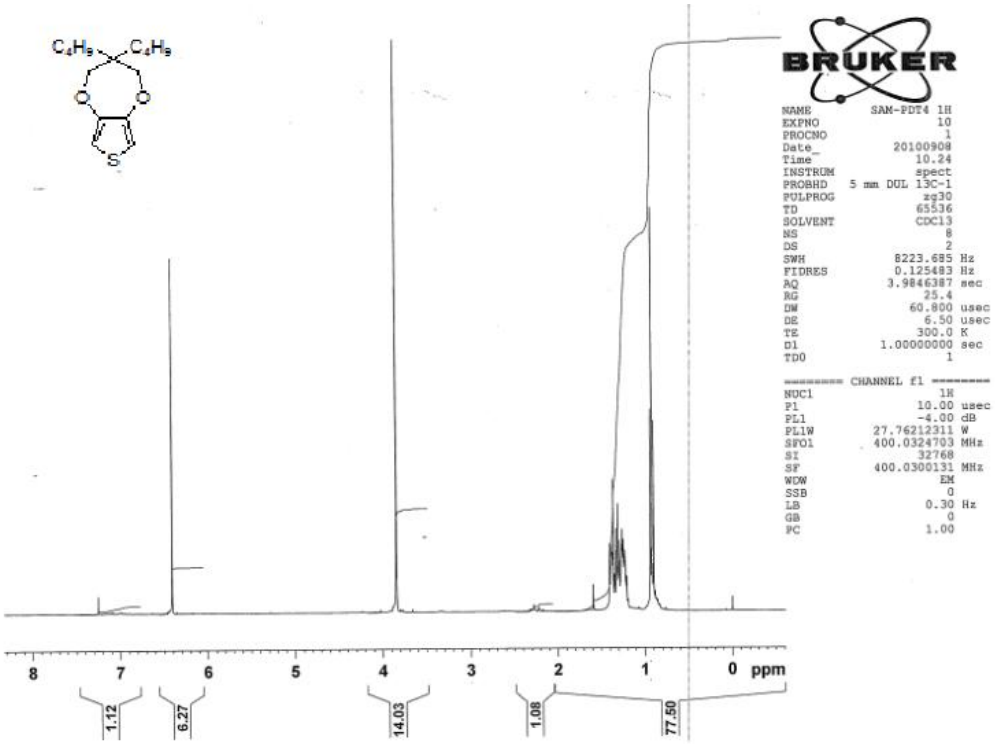

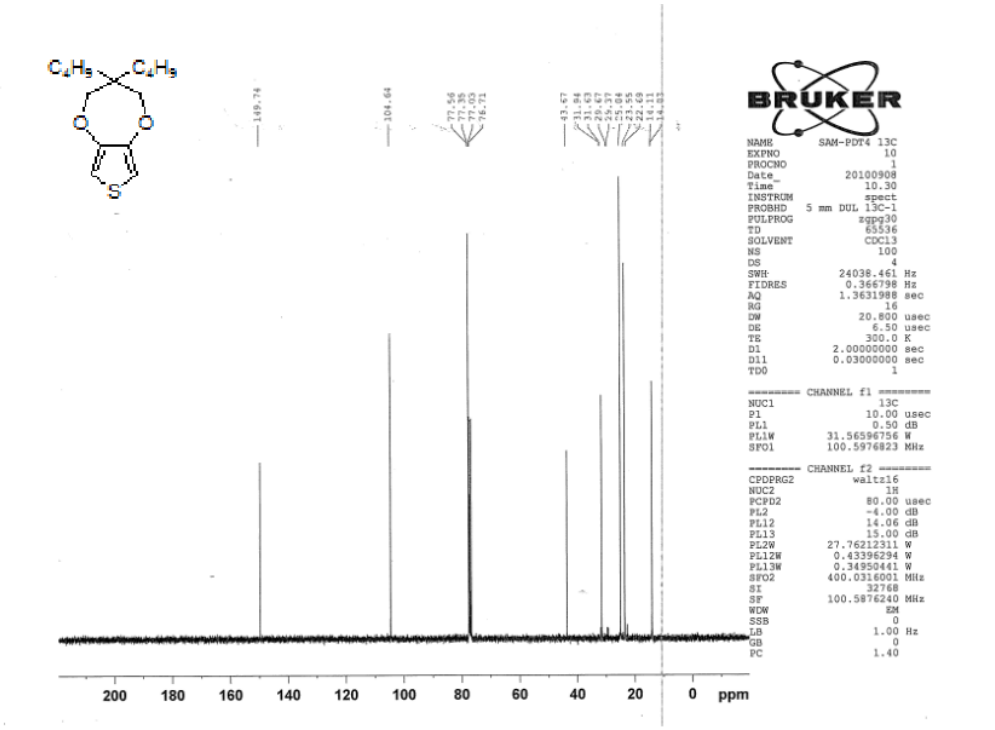

Figure B.4. ^{1}H NMR and ^{13}C NMR of ProDOT-C_4.

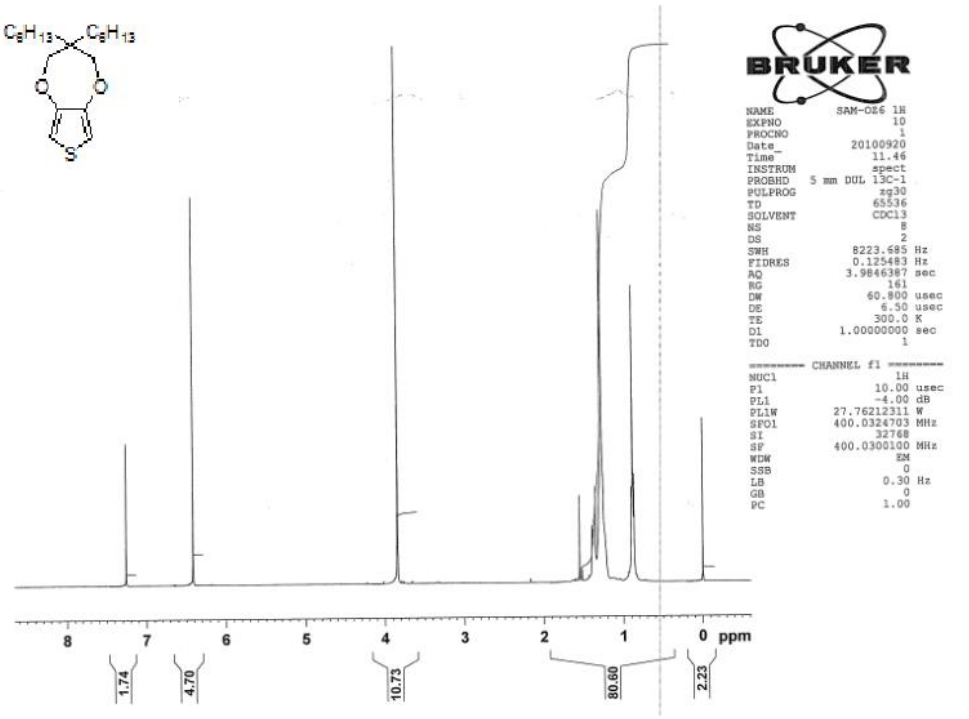

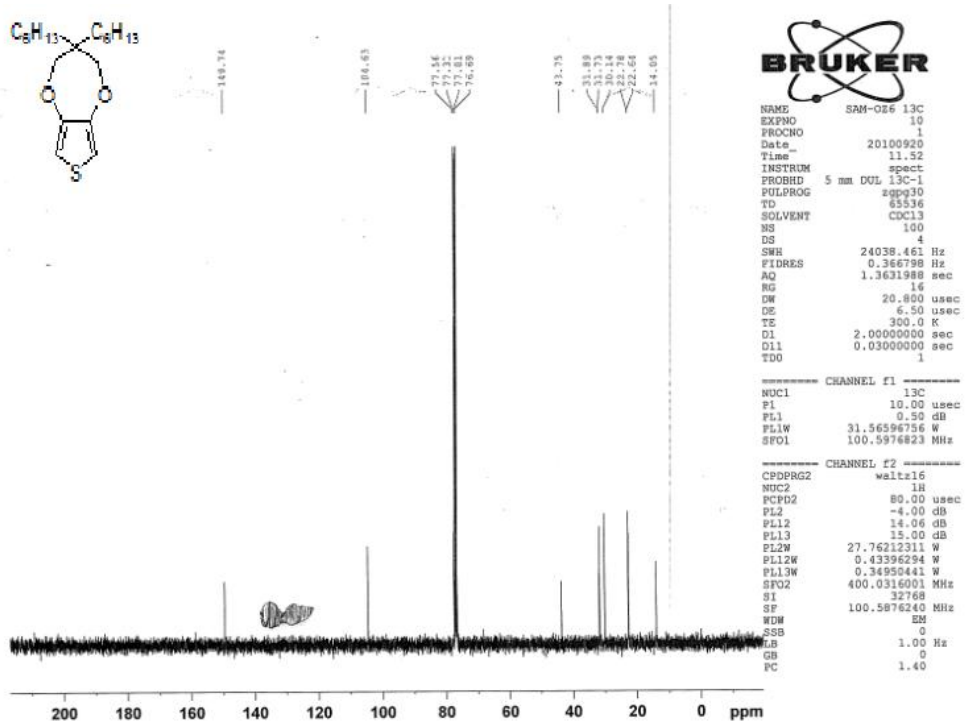

Figure B.5. ^{1}H NMR and ^{13}C NMR of ProDOT-C_6.

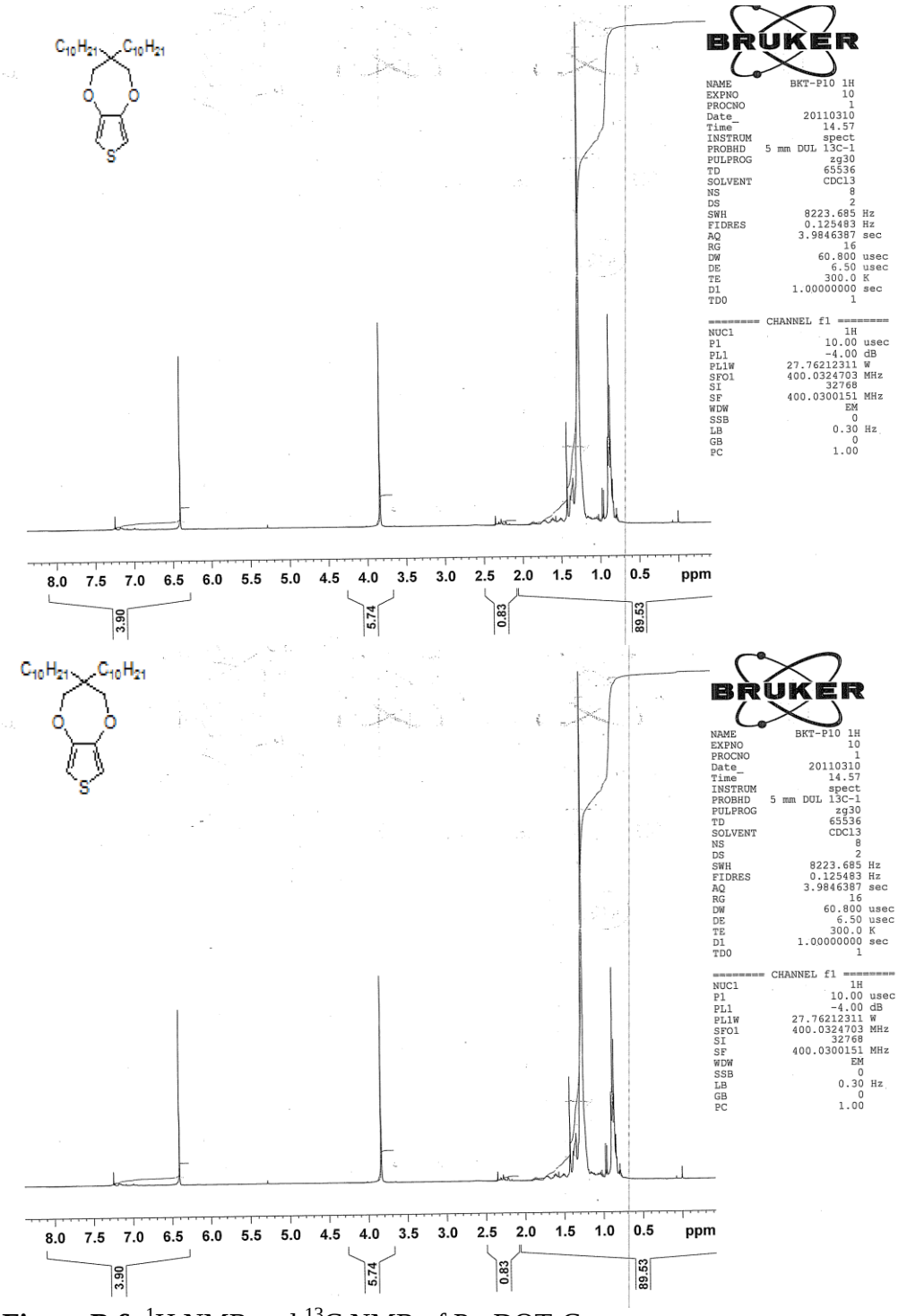

Figure B.6. ^{1}H NMR and ^{13}C NMR of ProDOT-C_{10}.